IEEE Access
Multidisciplinary ⋮ Rapid Review ⋮ Open Access Journal

Received March 23, 2018, accepted April 28, 2018, date of publication May 4, 2018, date of current version August 20, 2018.

*Digital Object Identifier 10.1109/ACCESS.2018.2833423*

# Cascaded $\alpha - \mu$ Fading Channels: Reliability and Security Analysis

**LONG KONG[1], (Graduate Student Member, IEEE), GEORGES KADDOUM[1], (Member, IEEE), AND DANIEL BENEVIDES DA COSTA[2], (Senior Member, IEEE)**

[1]Lab LaCIME, Department of Electrical Engineering, École de Technologie Supérieure, Université du Québec, Montréal, H3C 1K3, Canada
[2]Federal University of Ceará, Sobral-CE 62010-560, Brazil

Corresponding author: Long Kong (long.kong.1@ens.estmtl.ca)

This work was supported by the ÉTS Research Chair of Physical Layer Security in Wireless Networks.

**ABSTRACT** In this paper, the cascaded $\alpha - \mu$ fading distribution is first introduced and mathematically characterized, which arises as a generalization of the cascaded Rayleigh, Weibull, and Nakagami-*m* fading distribution, by properly selecting fading parameters $\alpha$ and $\mu$ with specific values. In particular, the statistical characterization of the cascaded $\alpha - \mu$ fading channels, namely, the probability density function and cumulative distribution function, are first studied. This set of new statistical results is applied to the modeling and analysis of the reliability and security performance of wireless communication systems over the cascaded $\alpha - \mu$ fading channel. Regarding system reliability, the amount of fading, outage probability, average channel capacity, and the average symbol error probability with coherent and non-coherent demodulation schemes are derived with respect to the univariate Fox's $H$-function. In terms of security analysis, the secrecy outage probability $\mathcal{P}_{\text{out}}$, the probability of non-zero secrecy capacity $\mathcal{P}_{\text{nz}}$, and the average secrecy capacity are analyzed in the exact closed-form expressions which are derived in the presence of an active eavesdropper. In addition, an asymptotic analysis of all aforementioned metrics is carried out, in order to gain more insights of the effect of the key system parameters on the reliability and security. Tractable results are computed in terms of the Fox's $H$-function and later on are successfully validated through Monte-Carlo simulations.

**INDEX TERMS** Cascaded $\alpha - \mu$ fading channels, Fox's $H$-function, reliability, secrecy analysis.

## I. INTRODUCTION

The ever-increasing demand for highly reliable wireless communication systems has led to the prosperous of various accurate channel modeling in system design and evaluation. A comprehensive summary of all existing fading models includes (i) short-term fading: Rayleigh, Rician, Nakagami-*m*, and Weibull; (ii) long-term fading: Log-normal; (iii) composite fading: Rayleigh-lognormal; and (iv) cascaded fading [1]–[8]. In particular, the cascaded fading channel is mathematically based on the multiplicative modeling approach and happens over wireless communication links when 1) transmitter-and-receiver pairs experience rich scattering, but the existence of some keyholes or pinholes makes it still possible to keep the transmission; 2) the received signals are engendered by the product of a bunch of rays reflected via $N$ statistically independent scatters.

### A. BACKGROUND AND RELATED WORKS

Along the years, the use of cascaded fading channels has shown applicability in the modeling of several scenarios such as multi-hop cooperative communications [9], [10], mobile-to-mobile (M2M) transmission channel [7], [11], [12], dual-hop fading channels, radio-frequency identification (RFID) pinhole channels [13], and multiple-input-multiple-output (MIMO) keyhole communication systems [2], [10], [14].

Specifically, for M2M communication system, the double Rayleigh distribution was proposed to model it [7], [12], [15]. Later on, in [7] and [15], a vehicle-to-vehicle (V2V) communication scenario was investigated by characterizing the wireless links, via the $N*$Nakagami-*m* distribution. As shown in [1], the $N*$Nakagami-*m* distribution is structured on the basis of the product of $N$ independent, but not necessarily identical distributed Nakagami-*m* random variables (RVs). Its statistics, including the probability density function (PDF) and cumulative distribution function (CDF), were derived in [1] as closed-form expressions, in terms of Meijer's $G$-function. The derived first-order statistics are particularly beneficial when evaluating the performance of the aforementioned various wireless communication scenarios over cascaded Nakagami-*m* fading channels. In addition, it is noted that the $N$*Nakagami-$m$ distribution can be reduced to double Rayleigh by attributing $m_1 = m_2 = 1$, where $m_1$ and $m_2$ represent the fading parameters of the respective channels. However, when accounting for both short- and long-term fading effects, the $N$*Nakagami-$m$ and $N$*Weibull distributions [4] cannot be adopted to model both fading impairments. As a consequence, the cascaded generalized $K$ distribution [3], [5] was put forth to model the composite fading/shadowing channels due to the lack of closed-form expressions for the statistics of other distributions, like Suzuki [7], [16], [17].

More recently, Yacoub [18] proposed in the $\alpha-\mu$ (or, equivalently, generalized gamma) distribution to model the small scale variation of fading signal under line-of-sight conditions. It is physically described with two key fading parameters, i.e., non-linearity of the propagation medium $\alpha$ and the clustering of the multipath waves $\mu$. This fading distribution has been examined applicable in vehicle communication [19] and on-body communication networks [20]. In additon, the $\alpha-\mu$ distribution encompasses as special cases of some well-known distributions, such as Rayleigh ($\alpha = 2, \mu = 1$), Weibull ($\alpha$ is the fading parameter, $\mu = 1$), and Nakagami-m ($\alpha = 2$, $\mu$ is the fading parameter) distribution, by setting appropriate fading parameters to specific values. Later on, the statistical characterization of the product of $\alpha-\mu$ variates, including its PDF and CDF, were investigated in [21]–[27], and the number of integers was extended from 2 to arbitrary N. The seminal results presented in [21] were given in terms of Fox's $H$-function. Since the Fox's $H$-function is an extremely general function, taking the shape of the Mellin-Barnes integral [28, eq. (1.2)]. It can also be extended to Meijer's $G$-function. However, the PDF and CDF of the product of $\alpha-\mu$ variates given in terms of hypergeometric functions is fairly complex in [23]; it renders its adoption in the performance analysis of wireless communication systems. Inspired from [21] and [23], the objective of this paper is to regenerate the cascaded $\alpha-\mu$ distribution in terms of Fox's $H$-function, due to its general form and feasible implementation in MATLAB, Mat hematica and Python.[1]

### B. CONTRIBUTIONS

Our analysis of cascaded $\alpha-\mu$ fading channel in wireless networks will be performed in terms of reliability and security. It is noteworthy that apart from analyzing the popular average bit error ratio performance, plenty of research attention concerning the security issue is also gained when designing a secure and reliable communication system. The security issue is based on Wyner's wiretap model [32], where the legitimate links are endangered by the malicious eavesdroppers. In the existing technical works [33]–[36], the authors studied the security problem over $\alpha-\mu$ fading channels from the perspective of information theory, in which the secrecy outage probability, the probability of non-zero secrecy capacity, and average secrecy capacity were characterized, respectively. However, no work in the open literature focused on cascaded $\alpha-\mu$ fading channels.

To this end, this paper aims to provide a reliability and security analysis of communications systems over cascaded $\alpha$-$\mu$ fading channels. The main contributions can be summarized as follows:

- The cascaded $\alpha-\mu$ distribution is first introduced. Its PDF and CDF are analyzed by first expressing the $\alpha-\mu$ distribution in terms of the Fox's $H$-function, and subsequently being derived by utilizing the property of the Fox's $H$-function distribution. In addition, other elementary statistics, including moments and moment-generating function (MGF), are also derived.
- The derived statistics are employed in the investigation of multi-hop relaying wireless systems with amplify-and-forward (AF) protocol over the cascaded $\alpha-\mu$ fading channel. In particular:
  - In the absence of eavesdroppers, the reliability of point-to-point wireless systems is characterized. Specifically, the amount of fading (AoF), the outage probability, the average channel capacity and the average symbol error probability (ASEP) are evaluated in terms of the univariate Fox's $H$-function.
  - In the presence of eavesdroppers, the physical layer security is investigated, where the secrecy outage probability (SOP), the probability of non-zero secrecy capacity (PNZ), and the average secrecy capacity are characterized and closed-form expressions in terms of the bivariate and univariate Fox's $H$-functions, are obtained.
  - Asymptotic behavior of all the aforementioned metrics are analyzed to gain further insights on the effect of the key system parameters on the overall performance. In addition, numerical results are conducted to confirm our analysis for both scenarios, perfect agreements are observed to show the accuracy and feasibility of our analysis in the field of wireless communication systems.
- The useful insight provided in our paper lies in the essence of the cascaded $\alpha-\mu$ fading channels, which can be reduced to several well-known cascaded fading channels, such as the cascaded Rayleigh, Weibull, Nakagami-$m$ fading channels by fixing $\alpha$ and $\mu$ with special values, furthermore, the exact closed-form expression of the PDF and CDF of the cascaded $\alpha-\mu$ distribution makes it tractable to grasp the behavior of reliability and security analysis for multi-hop wireless communication systems.

The rest of this paper is organized as follows. In Section II, the statistical characterization of cascaded $\alpha-\mu$ fading channel is first performed. Section III demonstrates the application

[1]The implementation of the univariate, bivariate or multivariate Fox's $H$-function are reported in [2] and [29]–[31] at Mathematica, MATLAB or Python. More specifically, the univariate Fox's $H$-function is implemented at Mathematica in [2] and [29], and at MATLAB in [30], whereas the implementation of the bivariate Fox's $H$-function is given at MATLAB in [31].

of cascaded $\alpha-\mu$ fading channels in modeling wireless communication systems, and performance metrics including the outage probability, average channel capacity and the average symbol error probability (ASEP) are analyzed respectively. In Section IV, the physical layer security of wireless communication systems over cascaded $\alpha$-$\mu$ fading channels is investigated, and performance metrics including the secrecy outage probability, the probability of non-zero secrecy capacity, and average secrecy capacity, are provided. Section V presents some illustrative numerical results along with insightful discussions. Concluding remarks and future works are outlined in Section VI.

*Notations:* $\Gamma(x)$ denotes the Gamma function [37, eq. (8.310.1)], $\Gamma(a,x)$ is the upper incomplete gamma function, $H^{m,n}_{p,q}[.]$ is the univariate Fox's $H$-function [28, eq. (1.2)], $H^{0,n:m_1,n_1:m_2,n_2}_{p,q:p_1,q_1:p_2,q_2}$ is the bivariate Fox's $H$-function [28, eq. (2.56)]. erfc(.) is the complementary error function. $\mathcal{B}(x,y)$ is the Beta function [37, eq. (8.380.1)]. $\psi(\cdot)$ is the digamma function. $G^{m,n}_{p,q}[.]$ is the Meijer's $G$-function [37, eq. (7.811.1)]. $\mathcal{M}[f(x),s]$ denotes the Mellin transform of $f(x)$ [38, eq. (8.2.5)], $\mathbb{E}(\cdot)$ and $\mathbb{V}(\cdot)$ mean expectation and variance, respectively. $\mathrm{Res}[f(x),p]$ represents the residue of function $f(x)$ at pole $x=p$.

## II. SYSTEM MODEL AND STATISTICAL CHARACTERIZATION

Let $Z$ be the product of $M$, $M\geq 1$ independently $\alpha-\mu$ distributed random variables (RVs) having parameters $(\alpha_i,\mu_i)$, i.e., $Z=\prod_{i=1}^{M}R_i$, the PDF of $R_i$ is given by [18]

$$f_{R_i}(r_i)=\frac{\alpha_i\mu_i^{\mu_i}r_i^{\alpha_i\mu_i}-1}{\Omega_i^{\alpha_i\mu_i}\Gamma(\mu_i)}\exp\left(-\mu_i\left(\frac{r_i}{\Omega_i}\right)^{\alpha_i}\right)$$
$$=\tau_i H^{1,0}_{0,1}\left[\upsilon_i r_i\,\middle|\,\begin{matrix}-\\(\mu_i-\frac{1}{\alpha_i},\frac{1}{\alpha_i})\end{matrix}\right],\tag{1}$$

where $\tau_i=\frac{\mu_i^{\frac{1}{\alpha_i}}}{\Omega_i\Gamma(\mu_i)}$, $\upsilon_i=\frac{\mu_i^{\frac{1}{\alpha_i}}}{\Omega_i}$, $\Omega_i=\frac{\Gamma(\mu_i)}{\Gamma(\mu_i+\frac{2}{\alpha_i})}$, the last step holds by using [28, eq. (1.125)].

*Theorem 1: The PDF of Z is given by*

$$f_Z(z)=\mathcal{D}_M H^{M,0}_{0,M}\left[\mathcal{V}_M z\,\middle|\,\begin{matrix}-\\\epsilon_1,\cdots,\epsilon_M\end{matrix}\right],\tag{2}$$

*where* $\mathcal{D}_M=\prod_{i=1}^{M}\tau_i$, $\mathcal{V}_M=\prod_{i=1}^{M}\upsilon_i$, $\epsilon_i=(\mu_i-\frac{1}{\alpha_i},\frac{1}{\alpha_i})$.

*Proof:* By using [39, eq. (3.12)], the proof is easily obtained. ∎

### A. SYSTEM MODEL

Suppose a wireless multi-hop amplify-and-forward relaying communication link, shown in Fig. 1, over cascaded $\alpha-\mu$ fading channel. It is assumed that each hop undergoes the $\alpha-\mu$ fading with fading coefficient $h_i$, and $h_i$ is characterized with fading parameters $\alpha_i$ and $\mu_i$. The instantaneous received signal-to-noise ratio (SNR) at the desired destination is expressed as

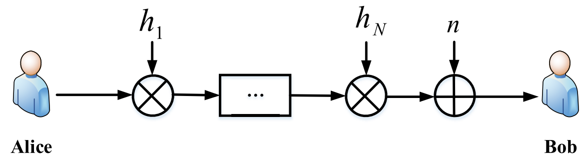


**FIGURE 1.** **Cascaded fading channels with $N$ components.**

$$\gamma=\prod_{i=1}^{N}\bar{\gamma}g_i,\tag{3}$$

where $\bar{\gamma}$ is the average power at the receiver side, $g_i=|h_i|^2$, and $h_i$ is the fading coefficient, which follows independent and non-identically $\alpha-\mu$ distribution with parameters $(\alpha_i,\mu_i)$. It is assumed that all $h_i$ are statistically independent, but not necessarily identically distributed. The PDF of $g_i$ is defined in [34] and [36, eq. (2)]given by

$$f_g(g_i)=\frac{\alpha_i g_i^{\frac{\alpha_i\mu_i}{2}-1}}{2\Omega_i^{\frac{\alpha_i\mu_i}{2}}\Gamma(\mu_i)}\exp\left[-\left(\frac{g_i}{\Omega_i}\right)^{\frac{\alpha_i}{2}}\right]$$
$$\overset{(a)}{=}\kappa_i H^{1,0}_{0,1}\left[\lambda_i g_i\,\middle|\,\begin{matrix}-\\\Phi_i\end{matrix}\right],\tag{4}$$

where $\Omega_i=\frac{\Gamma(\mu_i)}{\Gamma(\mu_i+\frac{2}{\alpha_i})}$, $\kappa_i=\frac{1}{\Omega_i\Gamma(\mu_i)}$, $\lambda_i=\frac{1}{\Omega_i}$, and $\Phi_i=(\mu_i-\frac{2}{\alpha_i},\frac{2}{\alpha_i})$. Step $(a)$ is derived by using [28, eq. (1.125)].

### B. STATISTICAL CHARACTERIZATION

*Theorem 2: The PDF and CDF of the instantaneous SNR defined in (3) can be expressed as*

$$f_\gamma(\gamma)=\mathcal{K}_N H^{N,0}_{0,N}\left[\mathcal{C}\gamma\,\middle|\,\begin{matrix}-\\\Phi_1,\cdots,\Phi_N\end{matrix}\right],\tag{5a}$$

$$F_\gamma(\gamma)=1-\frac{\mathcal{K}_N}{\mathcal{C}}H^{N+1,0}_{1,N+1}\left[\mathcal{C}\gamma\,\middle|\,\begin{matrix}(1,1)\\(0,1),\theta_1,\cdots,\theta_N\end{matrix}\right]$$
$$=1-\bar{F}_\gamma(\gamma),\tag{5b}$$

*where* $\mathcal{K}_N=\frac{\prod_{i=1}^{N}\kappa_i}{\bar{\gamma}}$, $\mathcal{C}=\frac{\prod_{i=1}^{N}\lambda_i}{\bar{\gamma}}$, $\theta_i=(\mu_i,\frac{2}{\alpha_i})$, *and* $\bar{F}_\gamma$ *is the complementary CDF (CCDF) of* $F_\gamma$.

*Proof:* Let $Z$ be the product of $N$ mutually independent and non-identically random variables (RVs) $g_1,g_2,\cdots,g_N$, that is

$$Z=\frac{\gamma}{\bar{\gamma}}=\prod_{i=1}^{N}g_i.\tag{6}$$

Since $\alpha$-$\mu$ distribution is a special case of the Fox's $H$-function distribution, by using the transformation property of Fox's $H$-function [39, eq. (3.12)] and $f_\gamma(\gamma)=\frac{1}{\bar{\gamma}}f_Z\left(\frac{z}{\bar{\gamma}}\right)$, the proof for (5a) is easily obtained. Afterwards, by applying [39, eq. (3.7)], the CDF is subsequently achieved. ∎

*Remark 1: The PDF of the ratio of two instantaneous SNRs,* $Y=\frac{\gamma_1}{\gamma_2}$, *respectively defined in (3),*

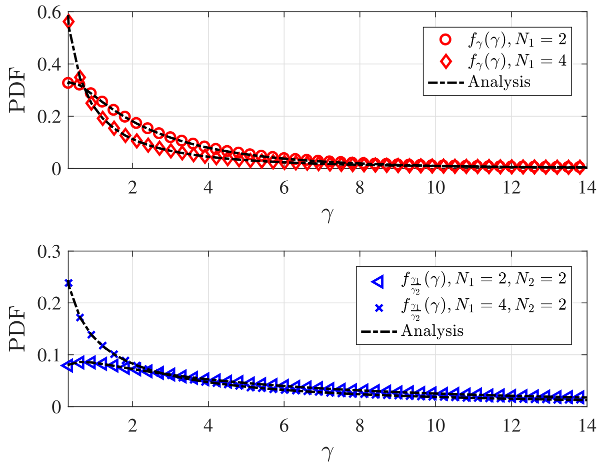


**FIGURE 2.** PDFs of $\gamma = \prod_{k=1}^{N} \bar{\gamma} g_k$ and the ratio of $\gamma = \frac{\gamma_1}{\gamma_2}$, where $\gamma_1 = \prod_{k=1}^{N_1} \bar{\gamma}_1\, g_{1,i}$, $\gamma_2 = \prod_{i=1}^{N_2} \bar{\gamma} g_{2,i}$, $g_k$, $g_{1,i}$, $g_{2,i}$ are implemented by using the WAFO toolbox [40] when $\bar{\gamma} = \bar{\gamma}_1 = 5$ dB and $\bar{\gamma}_2 = -5$ dB.

*i.e.,* $\gamma_1 = \prod_{i=1}^{N_1} \bar{\gamma}_1\, g_{1,i}$, *and* $\gamma_2 = \prod_{i=1}^{N_2} \bar{\gamma}_2\, g_{2,i}$ *is given by*

$$f_{\frac{\gamma_1}{\gamma_2}}(y) = \frac{\mathcal{K}_{N_1}\mathcal{K}_{N_2}}{\mathcal{C}_{N_2}^2} H_{N_2,N_1}^{N_1,N_2}\left[\frac{\mathcal{C}_{N_1}}{\mathcal{C}_{N_2}} y \,\middle|\, \begin{matrix} \Theta_1, \cdots, \Theta_{N_2} \\ \Phi_1, \cdots, \Phi_{N_1} \end{matrix}\right], \quad (7)$$

*where* $\Theta_n = \left(1 - \mu_i - \frac{2}{\alpha_i}, \frac{2}{\alpha_i}\right)$, $n = 1, \cdots, N_2$.

*Proof:* Using [39, eq. (3.14)], and after some simple mathematical manipulations, the proof is easily achieved. ■

As shown in Fig. 2, examples of PDFs for (5a) and (7) are plotted, one can observe that there is a perfect match between the Monte-Carlo simulation results and our analysis.

For the conveniences of the following performance analysis, the definition of Mellin transform for a continuous function $f(x)$ is recalled, which is given by

$$\mathcal{M}[f(x), s] = \int_0^\infty f(x) x^{s-1} dx. \quad (8)$$

Likewise, the Mellin transform for (5a) is straightforward given from [28, eq. (2.8)]

$$\mathcal{M}[f_\gamma(\gamma), s] = \frac{\mathcal{K}_N \prod_{i=1}^{N} \Gamma\left(\mu_i - \frac{2}{\alpha_i} + \frac{2}{\alpha_i}s\right)}{\mathcal{C}_N^s}. \quad (9)$$

### C. MOMENTS AND MGF

The $n$-th moment of the instantaneous SNR can be derived from the following definition,

$$\mathbb{E}[\gamma^n] = \int_0^\infty x^n f_\gamma(x) dx, \quad (10)$$

it can be achieved by using the Mellin transform of the Fox's $H$-function [41, eq. (2.25.2.1)], and thus given by

$$\mathbb{E}[\gamma^n] = \frac{\mathcal{K}_N \prod_{i=1}^{N} \Gamma\left(\mu_i + \frac{2}{\alpha_i}n\right)}{\mathcal{C}_N^{n+1}}. \quad (11)$$

Likewise, the MGF of the received SNR $\gamma$, is defined by

$$\mathbb{M}_\gamma(-s) = \int_0^\infty \exp(-xs) f_\gamma(x) dx, \quad (12)$$

it can be derived by re-expressing the $\exp(\cdot)$ function through its Fox's $H$-function form [41], namely,

$$\exp(-x) = H_{0,1}^{1,0}\left[x \,\middle|\, \begin{matrix} - \\ (0, 1) \end{matrix}\right],$$

and then making use of the Mellin transform of the product of two Fox's $H$-functions [41, eq. (2.25.1.1)], yields

$$\mathbb{M}_\gamma(-s) = \frac{\mathcal{K}_N}{s} H_{1,N}^{N,1}\left[\frac{\mathcal{C}}{s} \,\middle|\, \begin{matrix} (0, 1) \\ \Phi_1, \cdots, \Phi_N \end{matrix}\right]. \quad (13)$$

## III. RELIABILITY ANALYSIS OVER CASCADED $\alpha-\mu$ FADING CHANNELS

In this section, the objective is to evaluate the link performance, as shown in Fig. 1, when no eavesdropper is taken into account. The AoF, the outage probability, average channel capacity, and average symbol error probability are analyzed and derived in terms of the univariate Fox's $H$-function, respectively. In addition, their asymptotic behavior is given by using the residue approach given in [10, Sec. IV].

### A. AMOUNT OF FADING

The AoF is defined as the ratio of the variance to the square average SNR, and then using (11), we have

$$AF = \frac{\mathbb{V}(\gamma)}{\mathbb{E}^2(\gamma)} = \frac{\mathbb{E}(\gamma^2)}{\mathbb{E}(\gamma)^2} - 1 = \frac{\mathcal{C}_N}{\mathcal{K}_N}\frac{\prod_{i=1}^{N}\Gamma\left(\mu_i + \frac{4}{\alpha_i}\right)}{\prod_{i=1}^{N}\Gamma\left(\mu_i + \frac{2}{\alpha_i}\right)^2} - 1. \quad (14)$$

### B. OUTAGE PROBABILITY

The outage event happens when the output SNR falls below a given threshold $\gamma_{th}$, which can be expressed mathematically as

$$\mathcal{P}_{op}(\gamma_{th}) = Pr(\gamma < \gamma_{th}). \quad (15)$$

#### 1) EXACT ANALYSIS

By applying (5b), the outage probability is given by

$$\mathcal{P}_{op}(\gamma_{th}) = 1 - \frac{\mathcal{K}_N}{\mathcal{C}} H_{1,N+1}^{N+1,0}\left[\mathcal{C}\gamma_{th} \,\middle|\, \begin{matrix} (1, 1) \\ (0, 1), \theta_1, \cdots, \theta_N \end{matrix}\right]. \quad (16)$$

#### 2) ASYMPTOTIC ANALYSIS

When $\frac{\gamma_{th}}{\bar{\gamma}} \to \infty$, by using the residue approach, the asymptotic behavior of (16) is given by

$$\mathcal{P}_{op} \sim 1 - \frac{\mathcal{K}_N}{\mathcal{C}} \prod_{i=1}^{N} \Gamma(\mu_i). \quad (17)$$

*Proof:* See Appendix. A. ■

### C. AVERAGE CHANNEL CAPACITY

The average channel capacity over fading channels is computed by averaging the instantaneous channel capacity

$$\bar{C} = \int_0^\infty \log_2(1+\gamma) f_\gamma(\gamma) d\gamma. \tag{18}$$

#### 1) EXACT ANALYSIS

*Theorem 3: The average channel capacity over cascaded $\alpha-\mu$ fading channels is given by*

$$\bar{C} = \frac{\mathcal{K}_N}{\mathcal{C}\ln(2)} H^{N+2,1}_{2,N+2}\left[\mathcal{C}\left|\begin{matrix}(0,1),(1,1)\\(0,1),(0,1),\theta_1,\cdots,\theta_N\end{matrix}\right.\right]. \tag{19}$$

*Proof:* By applying the Parseval's relation for the Mellin transform on (18), we have

$$\bar{C} = \frac{1}{2\pi j}\int_{\mathcal{L}} \mathcal{M}[\log_2(1+\gamma), 1-s]\mathcal{M}[f(\gamma), s]ds, \tag{20}$$

where $j=\sqrt{-1}$, $\mathcal{L}$ is the integration path from $\upsilon - j\infty$ to $\upsilon + j\infty$, $\upsilon$ is a constant, and

$$\mathcal{M}[\log_2(1+\gamma), 1-s] = \frac{\Gamma(2-s)\Gamma(s-1)\Gamma(s-1)}{\ln(2)\Gamma(s)}, \tag{21a}$$

$$\mathcal{M}[f(\gamma), s] = \mathcal{K}\prod_{i=1}^N \Gamma\left(\mu_i - \frac{2}{\alpha_i} + \frac{2}{\alpha_i}s\right)\mathcal{C}^{-s}. \tag{21b}$$

After plugging (21a) and (21b) into (20), leading to the following result

$$\begin{aligned}\bar{C} &= \frac{\mathcal{K}_N}{2\ln(2)\pi i}\int_{\mathcal{L}} \frac{\Gamma(2-s)\Gamma(s-1)\Gamma(s-1)}{\Gamma(s)} \\ &\quad\times \prod_{i=1}^N \Gamma\left(\mu_i - \frac{2}{\alpha_i} + \frac{2}{\alpha_i}s\right)\mathcal{C}^{-s}ds \\ &\overset{(b)}{=} \frac{\mathcal{K}_N}{\ln(2)} H^{N+2,1}_{2,N+2}\left[\mathcal{C}\left|\begin{matrix}(-1,1),(0,1)\\(-1,1),(-1,1),\Phi_1,\cdots,\Phi_N\end{matrix}\right.\right],\end{aligned} \tag{22}$$

where step $(b)$ is developed by applying the definition of univariate Fox's $H$-function, and subsequently using [28, eq. (1.60)], the proof is completed. ∎

#### 2) ASYMPTOTIC ANALYSIS

At high SNR regime, by using the residue approach [34, Sec. IV], (19) can be easily determined as

$$\bar{C} \sim \frac{\mathcal{K}_N \prod_{i=1}^N \Gamma(\mu_i)}{\mathcal{C}\ln(2)}\left[\sum_{i=1}^N \frac{2}{\alpha_i}\psi(\mu_i) - \ln(\mathcal{C})\right]. \tag{23}$$

### D. AVERAGE SYMBOL ERROR PROBABILITY (ASEP)

Apart from the aforementioned two metrics, the average symbol error probability is considered as another crucial criterion when designing reliable transmission system. It is defined as follows

$$\bar{\mathcal{P}}^k_{se} = \int_0^\infty \mathcal{P}^k_{se}(\gamma) f_\gamma(\gamma) d\gamma, \tag{24}$$

**TABLE 1.** **Values of $a, b$ for different modulation schemes by using coherent demodulation where $\mathcal{P}^C_{se} = a\,\mathrm{erfc}(\sqrt{b\gamma})$.**

| Modulation Scheme | a | b |
|---|---|---|
| BPSK | $\frac{1}{2}$ | 1 |
| BFSK | $\frac{1}{2}$ | $\frac{1}{2}$ |
| QPSK, 4-QAM | 1 | $\frac{1}{2}$ |
| M-QAM ($M \geq 4$) | $\frac{2(\sqrt{M}-1)}{\sqrt{M}}$ | $\frac{3}{2(M-1)}$ |

**TABLE 2.** **Values of $a, b$ for different modulation schemes by using non-coherent demodulation where $\mathcal{P}^N_{se} = a\exp(-b\gamma)$.**

| Modulation Scheme | a | b |
|---|---|---|
| BFSK | $\frac{1}{2}$ | $\frac{1}{2}$ |
| DBPSK | $\frac{1}{2}$ | 1 |

where $k \in \{C, N\}$, $\mathcal{P}_{se}(\gamma)$ is the conditional error probability with different generic expressions for coherent and non-coherent modulation schemes, which are listed in Tables. 1 and 2 [42], respectively.

#### 1) EXACT ANALYSIS

*Theorem 4: The average ASEP over cascaded $\alpha$-$\mu$ fading channels by using coherent and non-coherent demodulation are respectively given by*

- *Coherent Demodulation*

$$\bar{\mathcal{P}}^C_{se} = \frac{a\mathcal{K}}{\mathcal{C}\sqrt{\pi}} H^{N,2}_{2,N+1}\left[\frac{\mathcal{C}}{b}\left|\begin{matrix}(1,1),(\frac{1}{2},1)\\\theta_1,\cdots,\theta_N,(0,1)\end{matrix}\right.\right], \tag{25}$$

- *Non-coherent Demodulation*

$$\bar{\mathcal{P}}^N_{se} = \frac{a\mathcal{K}}{b} H^{N,1}_{1,N}\left[\frac{\mathcal{C}}{b}\left|\begin{matrix}(0,1)\\\Phi_1,\cdots,\Phi_N\end{matrix}\right.\right]. \tag{26}$$

*Proof:* Re-expressing $\mathcal{P}^C_{se}$ in terms of the Fox's $H$-function [41, eq. (8.4.14.2)], we have

$$\mathcal{P}^C_{se} = a\mathrm{erfc}(\sqrt{b\gamma}) = \frac{a}{\sqrt{\pi}} H^{2,0}_{1,2}\left[b\gamma\left|\begin{matrix}(1,1)\\(0,1),(\frac{1}{2},1)\end{matrix}\right.\right], \tag{27}$$

Next, applying the Parseval's relation for Mellin transform of (24), yields the following result

$$\begin{aligned}\bar{\mathcal{P}}^C_{se} &= \int_0^\infty \mathcal{P}^C_{se}(\gamma) f_\gamma(\gamma) d\gamma \\ &= \frac{a}{2\pi^{\frac{3}{2}} i}\int_{\mathcal{L}} \mathcal{M}[\mathrm{erfc}(\sqrt{b\gamma}), 1-s]\mathcal{M}[f_\gamma(\gamma), s]ds,\end{aligned} \tag{28}$$

where $\mathcal{M}[\mathrm{erfc}(\sqrt{b\gamma}), 1-s]$ can be obtained from [41, eq. (8.4.14.2)] and is given by

$$\mathcal{M}[\mathrm{erfc}(\sqrt{b\gamma}), 1-s] = \frac{\Gamma(1-s)\Gamma\left(\frac{3}{2}-s\right)}{\Gamma(2-s)} b^{-(1-s)}. \tag{29}$$

Subsequently, substituting (29) and (21b) into (28), and then applying the definition of Fox's $H$-function, we have

$$\begin{aligned}\bar{\mathcal{P}}_{se}^{C} &= \frac{a\mathcal{K}}{2b\pi^{\frac{3}{2}}i}\int_{\mathcal{L}}\frac{\Gamma(1-s)\Gamma\left(\frac{3}{2}-s\right)}{\Gamma(2-s)} \\ &\times\prod_{i=1}^{N}\Gamma\left(\mu_i-\frac{2}{\alpha_i}+\frac{2}{\alpha_i}s\right)\left(\frac{\mathcal{C}}{b}\right)^{-s}ds \\ &= \frac{a\mathcal{K}}{b\sqrt{\pi}}H_{2,N+1}^{N,2}\left[\frac{\mathcal{C}}{b}\middle|\begin{matrix}(0,1),(-\frac{1}{2},1)\\ \Phi_1,\cdots,\Phi_N,(-1,1)\end{matrix}\right]. \quad (30)\end{aligned}$$

Finally, using the property of Fox's $H$-function [28, eq. (1.60)], the proof for (25) is accomplished.

Regarding the proof for (26), by providing the Mellin transform for the exponential function [41, eq.(8.4.3.1)] as follows,

$$\mathcal{M}[\exp(-b\gamma),1-s]=\frac{\Gamma(1-s)}{b^{(1-s)}}, \quad (31)$$

and then following the same steps from (28) to (30), as such, the proof is achieved. ■

### 2) ASYMPTOTIC ANALYSIS

At high $\bar{\gamma}$ regime, the asymptotic behavior of (25) and (26) can be likely obtained as follows by following the same method as shown in Appendix. A [34]

- Coherent Demodulation

$$\bar{\mathcal{P}}_{se}^{C}\sim\frac{a\mathcal{K}\left(\frac{\mathcal{C}}{b}\right)^{\frac{\alpha_j\mu_j}{2}}}{\mu_j\sqrt{\pi}\mathcal{C}}\Gamma\left(\frac{1+\alpha_j\mu_j}{2}\right)\prod_{i=1,}^{N-1}\Gamma\left(\mu_i-\frac{\alpha_j}{\alpha_i}\mu_j\right), \quad (32)$$

- Non-coherent Demodulation

$$\bar{\mathcal{P}}_{se}^{N}\sim\frac{a\mathcal{K}\left(\frac{\mathcal{C}}{b}\right)^{\frac{\alpha_j\mu_j}{2}}}{\sqrt{\pi}\mathcal{C}}\Gamma\left(\frac{\alpha_j\mu_j}{2}\right)\prod_{i=1,}^{N-1}\Gamma\left(\mu_i-\frac{\alpha_j}{\alpha_i}\mu_j\right). \quad (33)$$

where $\alpha_j\mu_j=\min(\alpha_i\mu_i)$, $i=1,\cdots,N$.

## IV. SECRECY ANALYSIS OVER CASCADED $\alpha-\mu$ FADING CHANNELS

In this section, the security issue over cascaded $\alpha-\mu$ fading channels is analyzed from the information theoretical perspective. The classic Wyner's wiretap channel model is deployed, where a transmitter, named Alice, intends to communicate with the legitimate destination, Bob, whilst encountering a malicious wiretapper, Eve, over the cascaded $\alpha-\mu$ fading channels, a possible system configuration is shown in Fig. 3. It is assumed that (i) all users are equipped with a single antenna; (ii) they have perfect knowledge of their channel state information (CSI); (iii) the main channel is independent of the wiretap channel.

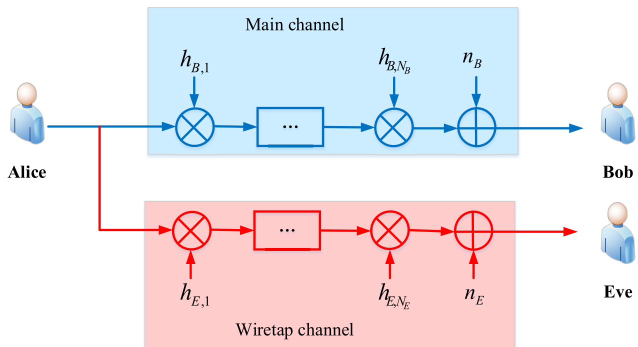


**FIGURE 3. Cascaded $\alpha-\mu$ fading channels in the presence of an active eavesdropper.**

### A. SYSTEM MODEL

Suppose a wireless legitimate link, from Alice to Bob, undergoes the cascaded fading channels while in the presence of an active Eve, where the channel coefficients are modeled by independent $\alpha$-$\mu$ distributions. The link between Alice and Bob is named as the main channel, whereas the one between Alice and Eve is called the wiretap channel. As a consequence, the instantaneous SNRs at Bob and Eve can be respectively expressed as

$$\gamma_B=\prod_{i=1}^{N_B}\bar{\gamma}_B g_{B,i}, \quad (34a)$$

$$\gamma_E=\prod_{j=1}^{N_E}\bar{\gamma}_E g_{E,j}, \quad (34b)$$

where $\bar{\gamma}_B=\frac{P}{\sigma_B}$ and $\bar{\gamma}_E=\frac{P}{\sigma_E}$, $g_{B,i}=|h_{B,i}|^2$, $g_{E,j}=|h_{E,j}|^2$, $P,\sigma_B$ and $\sigma_E$ are the transmission power at Alice, the noise power at Bob and Eve, respectively.

By deploying Theorem 2 on $\gamma_B$ and $\gamma_E$, $f_B(\gamma_B)$ and $f_E(\gamma_E)$ are respectively given by

$$f_B(\gamma_B)=\mathcal{K}_{N_B}H_{0,N_B}^{N_B,0}\left[\mathcal{C}_{N_B}\gamma_B\middle|\begin{matrix}-\\ \Phi_1,\cdots,\Phi_{N_B}\end{matrix}\right], \quad (35a)$$

$$f_E(\gamma_E)=\mathcal{K}_{N_E}H_{0,N_E}^{N_E,0}\left[\mathcal{C}_{N_E}\gamma_E\middle|\begin{matrix}-\\ \Theta_1,\cdots,\Theta_{N_E}\end{matrix}\right], \quad (35b)$$

where

$$\begin{cases}\mathcal{K}_{N_B}=\frac{\prod_{i=1}^{N_B}\kappa_{B,i}}{\bar{\gamma}_B}\\ \Phi_i=\left(\mu_{B,i}-\frac{2}{\alpha_{B,i}},\frac{2}{\alpha_{B,i}}\right) \qquad i=1,\cdots,N_B,\\ \mathcal{C}_{N_B}=\frac{\prod_{i=1}^{N_B}\lambda_{B,i}}{\bar{\gamma}_B},\end{cases}$$

and

$$\begin{cases}\mathcal{K}_{N_E}=\frac{\prod_{j=1}^{N_E}\kappa_{B,j}}{\bar{\gamma}_E}\\ \Theta_j=\left(\mu_{E,j}-\frac{2}{\alpha_{E,j}},\frac{2}{\alpha_{E,j}}\right) \qquad j=1,\cdots,N_E.\\ \mathcal{C}_{N_E}=\frac{\prod_{j=1}^{N_E}\lambda_{E,j}}{\bar{\gamma}_E},\end{cases}$$

According to [43], the instantaneous secrecy capacity is mathematically defined as the difference of the instantaneous capacity of the main channel and wiretap channel, given as follows

$$C_s = \begin{cases} C_M - C_W, & \gamma_B > \gamma_E \\ 0, & \text{otherwise.} \end{cases} \tag{36}$$

where $C_M = \log_2(1+\gamma_B)$, $C_W = \log_2(1+\gamma_E)$.

### B. SECRECY OUTAGE PROBABILITY

The secrecy outage probability $\mathcal{P}_{out}$ is defined as the probability with an instantaneous secrecy capacity, $C_s$, falling down the target secrecy rate $R_t$.

Revisiting (36), the secrecy outage probability $\mathcal{P}_{out}$ for the Wyner's wiretap fading model is conceptually explained through two cases: (i) $C_s < R_s$ whilst positive secrecy capacity is guaranteed; (ii) $P_{out}(R_s)$ definitely happens when the secrecy capacity is non-positive [44]. $\mathcal{P}_{out}(R_s)$ can thus be rewritten as follows:

$$\begin{aligned}
\mathcal{P}_{out}(R_t) &= \mathcal{P}r(C_s < R_t) \\
&= \mathcal{P}r(\gamma_B \le R_s\gamma_E + R_s - 1) \\
&= \mathcal{P}r(C_s < R_s|\gamma_B > \gamma_E)\mathcal{P}r(\gamma_B > \gamma_E) + \mathcal{P}r(\gamma_B < \gamma_E) \\
&= \int_0^\infty \int_{\gamma_E}^{\gamma_0} f_B(\gamma_B) f_E(\gamma_E) d\gamma_B d\gamma_E \\
&\quad + \int_0^\infty \int_0^{\gamma_E} f_B(\gamma_B) f_E(\gamma_E) d\gamma_B d\gamma_E \\
&= \int_0^\infty f_E(\gamma_E)\left[\int_0^{\gamma_0} - \int_0^{\gamma_E}\right] f_B(\gamma_B) d\gamma_B d\gamma_E \\
&\quad + \int_0^\infty \int_0^{\gamma_E} f_B(\gamma_B) f_E(\gamma_E) d\gamma_B d\gamma_E \\
&= \int_0^\infty F_B(\gamma_0) f_E(\gamma_E) d\gamma_E \\
&= 1 - \int_0^\infty \bar{F}_B(\gamma_0) f_E(\gamma_E) d\gamma_E,
\end{aligned} \tag{37}$$

where $\gamma_0 = 2^{R_t}\gamma_E + 2^{R_t} - 1 = R_s\gamma_E + \mathcal{W}$, $R_s = 2^{R_t}$, $\mathcal{W} = 2^{R_t} - 1$, and with the help of (5b), we have

$$\bar{F}_B(\gamma_0) = \frac{\mathcal{K}_{N_B}}{\mathcal{C}_{N_B}} H^{N_B+1,0}_{1,N_B+1}\left[\mathcal{C}_{N_B}\gamma_0 \left| \begin{matrix} (1,1) \\ (0,1), \theta_1, \cdots, \theta_{N_B} \end{matrix} \right.\right]. \tag{38}$$

#### 1) EXACT ANALYSIS

*Theorem 5: The secrecy outage probability over cascaded $\alpha-\mu$ wiretap fading channels, in the presence of non-colluding eavesdroppers, is given by (39), where $\bar{\Theta}_j = (1 - \mu_{E,j} + \frac{2}{\alpha_{E,j}}, \frac{2}{\alpha_{E,j}})$ and $\bar{\Phi}_i = (1-\mu_{B,i}, \frac{2}{\alpha_{B,i}})$, which is shown at the bottom of the next page.*

*Proof:* See Appendix. B. ∎

*Remark 2: The secrecy outage probability over cascaded $\alpha-\mu$ wiretap fading channels is lower bounded by*

$$\begin{aligned}
\mathcal{P}^L_{out} &= 1 - \frac{\mathcal{K}_{N_B}\mathcal{K}_{N_E}}{\mathcal{C}_{N_B}\mathcal{C}_{N_E}} \\
&\quad \times H^{N_B+1,N_E}_{N_E+1,N_B+1}\left[\frac{R_s\mathcal{C}_{N_B}}{\mathcal{C}_{N_E}} \left| \begin{matrix} \bar{\Theta}_1, \cdots, \bar{\Theta}_{N_E}, (1,1) \\ (0,1), \Phi_1, \cdots, \Phi_{N_B} \end{matrix} \right.\right].
\end{aligned} \tag{40}$$

*Proof:* As $\bar{\gamma}_E$ tends to $\infty$, it physically means that the eavesdropper is super close to the transmitter, the $\mathcal{P}_{out}$ is lower bounded by

$$\begin{aligned}
\mathcal{P}_{out} &= \mathcal{P}r(\gamma_B \le R_s\gamma_E + \mathcal{W}) \\
&\ge \underbrace{\mathcal{P}r(\gamma_B \le R_s\gamma_E)}_{\mathcal{P}^L_{out}} \\
&= 1 - \int_0^\infty \bar{F}_B(R_s\gamma_E) f_E(\gamma_E) d\gamma_E \\
&= 1 - \frac{\mathcal{K}_{N_B}\mathcal{K}_{N_E}}{\mathcal{C}_{N_B}} \int_0^\infty H^{N_E,0}_{0,N_E}\left[\mathcal{C}_{N_E}\gamma_E \left| \begin{matrix} - \\ \Theta_1, \cdots, \Theta_{N_E} \end{matrix} \right.\right] \\
&\quad \times H^{N_B+1,0}_{1,N_B+1}\left[\mathcal{C}_{N_B}R_s\gamma_E \left| \begin{matrix} (1,1) \\ (0,1), \Phi_1, \cdots, \Phi_{N_B} \end{matrix} \right.\right] d\gamma_E,
\end{aligned} \tag{41}$$

subsequently, the proof is achieved by using the Mellin transform of the product of two Fox's $H$-function [41, eq.(2.25.1.1)]. ∎

*Remark 3: When $\alpha_{B,i} = 2$, and $\alpha_{E,j} = 2$, by using the transformation between Meijer's G-function and Fox's H-function [41, eq.(8.3.2.21)], the asymptotic analysis of (40) can be further simplified as follows in terms of the Meijer's G-function [37, eq. (7.811.1)],*[2]

$$\begin{aligned}
\mathcal{P}^{Asy}_{out} &= 1 - \frac{\mathcal{K}_{N_B}\mathcal{K}_{N_E}}{\mathcal{C}_{N_B}\mathcal{C}_{N_E}} \\
&\quad \times G^{N_B+1,N_E}_{N_E+1,N_B+1}\left[\frac{R_s\mathcal{C}_{N_B}}{\mathcal{C}_{N_E}} \left| \begin{matrix} 1-\mu_{E,1}, \cdots, 1-\mu_{E,N_E}, 1 \\ 0, \mu_{B,1}, \cdots, \mu_{B,N_B} \end{matrix} \right.\right].
\end{aligned} \tag{42}$$

#### 2) ASYMPTOTIC ANALYSIS

By using the residue approach given in [10], the asymptotic behavior of $\mathcal{P}_{out}$ is given in Table. 3.

*Proof:* See Appendix. C. ∎

### C. PROBABILITY OF NON-ZERO SECRECY CAPACITY

Recalling the secrecy capacity over Wyner's wiretap channel, a non-zero secrecy capacity event happens when $\mathcal{C}_s$ is positive on the condition that $\gamma_B > \gamma_E$. By deploying the math language, it can be thus expressed as follows

$$\begin{aligned}
\mathcal{P}_{nz} &= Pr(C_s > 0) = Pr(\gamma_B > \gamma_E) \\
&= Pr\left(\frac{\gamma_E}{\gamma_B} < 1\right) = F_{\frac{\gamma_E}{\gamma_B}}(1).
\end{aligned} \tag{46}$$

[2]The implementation of the Meijer's $G$-function is available in mathematical packages, like Matlab2017b, Maple and Mathematica [45].

**TABLE 3.** Asymptotic analysis of the $\mathcal{P}_{out}$.

| Scenario | Asymptotic $\mathcal{P}_{out}$ |
|---|---|
| $\bar{\gamma}_E \to \infty$ | $1-\frac{\mathcal{K}_{N_B}\mathcal{K}_{N_E}}{\mathcal{C}_{N_B}\mathcal{C}_{N_E}}\left[\frac{\prod_{i=1}^{N_B}\Gamma\left(\mu_{B,i}+\frac{\alpha_{E,k}\mu_{E,k}}{\alpha_{B,i}}\right)\prod_{j=1}^{N_E-1}\Gamma\left(\mu_{E,j}-\frac{\alpha_{E,k}\mu_{E,k}}{\alpha_{E,j}}\right)}{\mu_E}\left(\frac{\mathcal{C}_{N_E}}{\mathcal{C}_{N_B}R_s}\right)^{\frac{\alpha_{E,k}\mu_{E,k}}{2}}\right],\quad (43)$ where $\alpha_{E,k}\mu_{E,k}=\min(\alpha_{E,1}\mu_{E,1},\cdots,\alpha_{E,j}\mu_{E,j}), j=1,\cdots,N_E$. |
| $\bar{\gamma}_B \to \infty$ | $\frac{\prod_{j=1}^{N_E}\Gamma\left(\mu_{E,j}+\frac{\alpha_{B,k}\mu_{B,k}}{\alpha_{E,j}}\right)\prod_{i=1}^{N_B-1}\Gamma\left(\mu_{B,i}-\frac{\alpha_{B,k}\mu_{B,k}}{\alpha_{B,i}}\right)}{\mu_{B,k}}\left(\frac{\mathcal{C}_{N_B}R_s}{\mathcal{C}_{N_E}}\right)^{\frac{\alpha_{B,k}\mu_{B,k}}{2}},\quad (44)$ where $\alpha_{B,k}\mu_{B,k}=\min(\alpha_{B,1}\mu_{B,1},\cdots,\alpha_{B,i}\mu_{B,i}), i=1,\cdots,N_B$. |
| $\bar{\gamma}_E \to 0$ | $1-\frac{\mathcal{K}_{N_B}}{\mathcal{C}_{N_B}}H_{1,N_B+1}^{N_B+1,0}\left[\frac{R_s\mathcal{C}_{N_B}}{\mathcal{C}_{N_E}}\middle\vert\begin{matrix}(1,1)\\(0,1),\theta_1,\cdots,\theta_{N_B}\end{matrix}\right],\quad (45)$ |
| $\bar{\gamma}_B \to 0$ | 1 |

### 1) EXACT ANALYSIS

*Theorem 6: The probability of non-zero secrecy capacity over cascaded $\alpha-\mu$ wiretap fading channels is given by*

$$\mathcal{P}_{nz}=1-\frac{\mathcal{K}_{N_B}\mathcal{K}_{N_E}}{\mathcal{C}_{N_B}\mathcal{C}_{N_E}}\times H_{N_B+1,N_E+1}^{N_E+1,N_B}\left[\frac{\mathcal{C}_{N_E}}{\mathcal{C}_{N_B}}\middle\vert\begin{matrix}\bar{\Phi}_1,\cdots,\bar{\Phi}_{N_B},(1,1)\\(0,1),\theta_1,\cdots,\theta_{N_E}\end{matrix}\right],\quad(47)$$

*where* $\theta_j=\left(\mu_{E,j},\frac{2}{\alpha_{E,j}}\right)$.

*Proof:* Recalling the Remark. 1, and subsequently applying [39, eq. (3.7)], the proof is completed. ■

Motivated by **Remark** 3, when $\alpha_{B,i}=2$, and $\alpha_{E,j}=2$, which means both the main and the wiretap channel undergo the Nakagami-$m$ fading, the $\mathcal{P}_{nz}$ is indeed over the cascaded Nakagami-$m$ wiretap fading channels, and it is thus given by

$$\mathcal{P}_{nz}=1-\frac{\mathcal{K}_{N_B}\mathcal{K}_{N_E}}{\mathcal{C}_{N_B}\mathcal{C}_{N_E}}\times G_{N_B+1,N_E+1}^{N_E+1,N_B}\left[\frac{\mathcal{C}_{N_E}}{\mathcal{C}_{N_B}}\middle\vert\begin{matrix}1-\mu_{B,1},\cdots,1-\mu_{B,N_B},1\\0,\mu_{E,1},\cdots,\mu_{E,N_E}\end{matrix}\right].\quad(48)$$

### 2) ASYMPTOTIC ANALYSIS

When $R_t=0$, $R_s=1$, in accordance with the definition of SOP and PNZ, we have

$$\begin{aligned}\mathcal{P}_{out}&=Pr(\gamma_E\le R_s\gamma_B+R_s-1)\\&=1-\underbrace{Pr(\gamma_B\ge\gamma_E)}_{\mathcal{P}_{nz}}.\end{aligned}\quad(49)$$

Consequently, the asymptotic behavior of the PNZ can be easily derived by making some simple algebraic substitutions.

## D. AVERAGE SECRECY CAPACITY

*Theorem 7: The average secrecy capacity over cascaded $\alpha-\mu$ wiretap fading channels is given by (50), shown at the bottom of next page, where* $D_i=\left(1-\mu_{B,i},\frac{2}{\alpha_{B,i}},\frac{2}{\alpha_{B,i}}\right)$, $E_j=\left(1-\mu_{E,j},\frac{2}{\alpha_{E,j}},\frac{2}{\alpha_{E,j}}\right)$, $\phi_i=\left(\mu_{B,i},\frac{2}{\alpha_{B,i}}\right)$, $H_{p,q:p_1,q_1:p_2,q_2}^{m,n:m_1,n_1:m_2:n_2}[.]$ *and* $H_{p,q}^{m,n}[.]$ *are the bivariate and univariate Fox's $H$-function [28, Eqs. (1.2) and (2.56)], respectively.*

*Proof:* See Appendix. D. ■

## V. NUMERICAL RESULTS AND DISCUSSIONS

In this section, we confirm the accuracy of our analytical derivations demonstrated in Sections III and IV, in comparison with Monte-Carlo simulation results.[3] For the conciseness of illustrations, the curves only with markers are the Monte-Carlo simulation outcomes, whereas the ones denoted with lines are used to depict our analytical results.

## A. RELIABILITY ANALYSIS OVER CASCADED $\alpha$-$\mu$ FADING CHANNELS

Considering the system configuration shown in Fig. 1, in Figs. 4-6, we plot the outage probability, the average channel capacity and the ASEP with coherent demodulation scheme over cascaded $\alpha-\mu$ fading channels, respectively. Those figures reveal that our derivations given by (16), (19) and (25) are in perfect match with simulation outcomes, which are particularly validated for several spe-

[3]It is worthy to mention that (i) the $\alpha-\mu$ fading channel is implemented by using the WAFO toolbox [40]; (ii) the implementation of the Fox's $H$-function is computationally practicable, the numerical evaluation of univariate and bivariate Fox's $H$-function of (39) and (40) for MATLAB implementations are based on the method proposed in [30, Table. II] and [31, Appendix. A], respectively.

$$\mathcal{P}_{out}(R_s)=1-\frac{\mathcal{K}_{N_B}\mathcal{K}_{N_E}\mathcal{W}}{\mathcal{C}_{N_B}R_s}H_{1,0;N_E,1;N_B,1}^{0,1;1,N_E;0,N_B}\left[\frac{R_s}{\mathcal{C}_{N_E}\mathcal{W}},\frac{1}{\mathcal{C}_{N_B}\mathcal{W}}\middle\vert\begin{matrix}(2,1,1)\\-\end{matrix}\middle\vert\begin{matrix}\bar{\Theta}_1,\cdots,\bar{\Theta}_{N_E}\\(1,1)\end{matrix}\middle\vert\begin{matrix}\bar{\Phi}_1,\cdots,\bar{\Phi}_{N_B}\\(0,1)\end{matrix}\right],\quad(39)$$

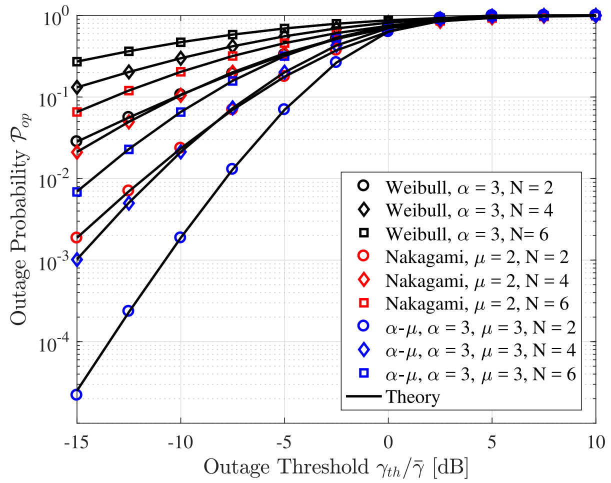


**FIGURE 4.** $\mathcal{P}_{op}$ **versus** $\gamma_{th}/\bar{\gamma}$ **over cascaded** $\alpha-\mu$ **wiretap fading channels for selected values of** $N$**.**

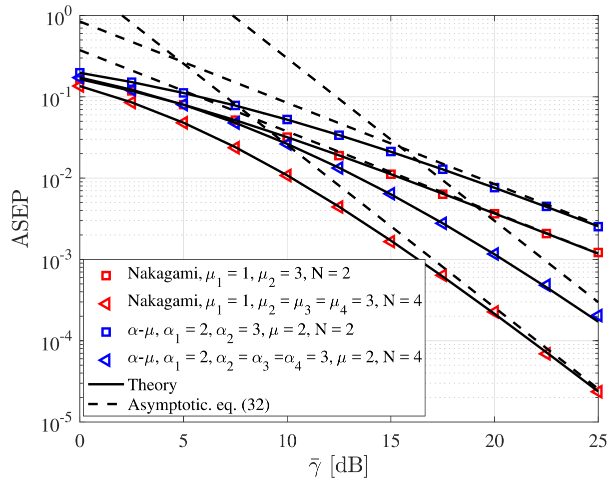


**FIGURE 6.** **The ASEP** $\bar{\mathcal{P}}_{se}^{C}$ **over cascaded** $\alpha-\mu$ **fading channels.**

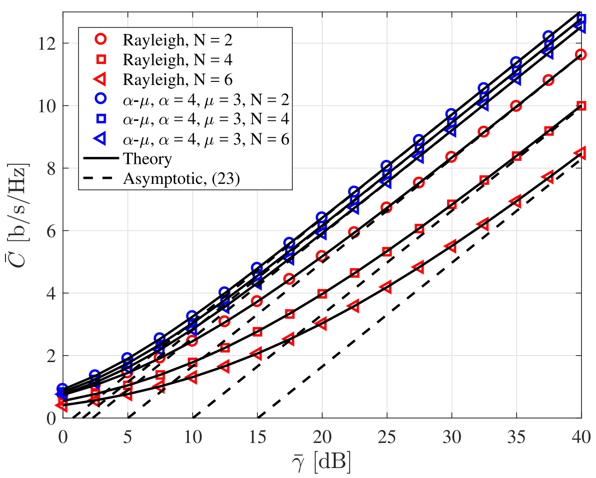


**FIGURE 5.** **Average channel capacity** $\bar{C}$ **over cascaded** $\alpha-\mu$ **fading channels.**

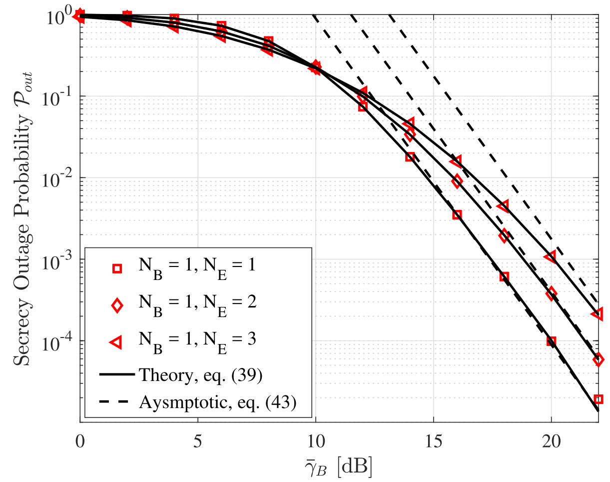


**FIGURE 7.** $\mathcal{P}_{out}$ **versus** $\bar{\gamma}_B$ **over cascaded** $\alpha-\mu$ **wiretap fading channels when** $\bar{\gamma}_E = 6$ **dB,** $R_s = 0.5$**,** $\alpha_B = 4$**,** $\mu_B = 2$**,** $\alpha_E = 2$**, and** $\mu_E = 3$**.**

cific cases, such as Rayleigh, Nakagami-$m$, and Weibull, respectively.

To terminate the reliability analysis over cascaded $\alpha-\mu$ fading channels, one can perceive the following conclusions from the three figures (i) the performance metrics physically demonstrate worse trend with the increase of $N$, outstandingly, it is caused by the fact that the multiplication of several successive fading makes it less likely to transmit the desired messages successfully; (ii) for a given fading scenario, reliable communication can be assured only by increasing the transmitting power.

$$\begin{aligned}\bar{C}_s = & \underbrace{\frac{\mathcal{K}_{N_B}\mathcal{K}_{N_E}}{\ln(2)\mathcal{C}_{N_B}\mathcal{C}_{N_E}} H^{0,N_B;1,2;N_E,1}_{N_B,0;2,2;1,N_E+1}\left[\frac{1}{\mathcal{C}_{N_B}},\frac{\mathcal{C}_{N_E}}{\mathcal{C}_{N_B}}\left|\begin{matrix}D_1,\cdots,D_{N_B}\\ -\end{matrix}\right|\begin{matrix}(1,1),(1,1)\\(1,1),(0,1)\end{matrix}\left|\begin{matrix}(1,1)\\ \theta_1,\cdots,\theta_{N_E},(0,1)\end{matrix}\right.\right]}_{\mathcal{I}_1} \\ & + \underbrace{\frac{\mathcal{K}_{N_B}\mathcal{K}_{N_E}}{\ln(2)\mathcal{C}_{N_B}\mathcal{C}_{N_E}} H^{0,N_E;1,2;N_B,1}_{N_E,0;2,2;1,N_B+1}\left[\frac{1}{\mathcal{C}_{N_E}},\frac{\mathcal{C}_{N_B}}{\mathcal{C}_{N_E}}\left|\begin{matrix}E_1,\cdots,E_{N_E}\\ -\end{matrix}\right|\begin{matrix}(1,1),(1,1)\\(1,1),(0,1)\end{matrix}\left|\begin{matrix}(1,1)\\ \phi_1,\cdots,\phi_{N_B},(1,1)\end{matrix}\right.\right]}_{\mathcal{I}_2} \\ & + \underbrace{\frac{\mathcal{K}_{N_E}}{\ln(2)\mathcal{C}_{N_E}} H^{1,2+N_E}_{2+N_E,2}\left[\frac{1}{\mathcal{C}_{N_E}}\left|\begin{matrix}(1,1),(1,1),\left(1-\mu_{E,l},\frac{2}{\alpha_{E,l}}\right),\cdots,\left(1-\mu_{E,N_E},\frac{2}{\alpha_{E,N_E}}\right)\\ (1,1),(0,1)\end{matrix}\right.\right]}_{\mathcal{I}_3}. \end{aligned} \quad (50)$$

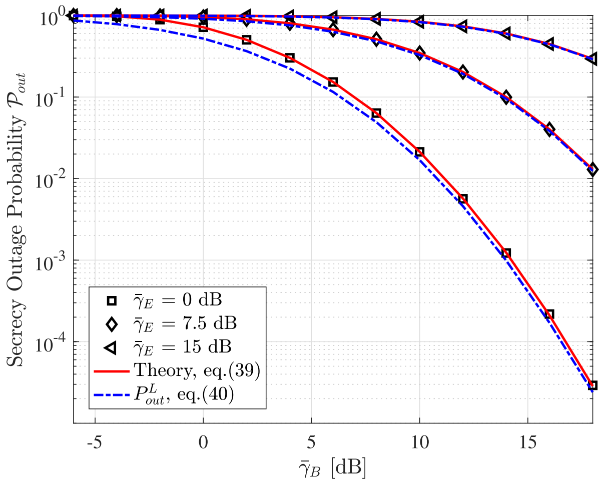


**FIGURE 8.** $\mathcal{P}_{out}$ **versus** $\bar{\gamma}_B$ **over cascaded** $\alpha-\mu$ **wiretap fading channels when** $N_B = N_E = 2$, $R_s = 0.5$, $\alpha_B = 4$, $\mu_B = 3$, $\alpha_E = 2$, **and** $\mu_E = 2$.

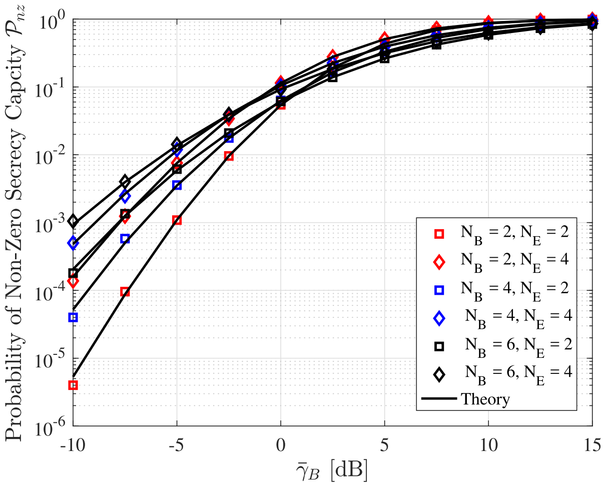


**FIGURE 9.** $\mathcal{P}_{nz}$ **versus** $\bar{\gamma}_B$ **over cascaded** $\alpha-\mu$ **wiretap fading channels when** $\bar{\gamma}_E = 5$ **dB,** $\alpha_B = 3$, $\mu_B = 2$, $\alpha_E = 2$, **and** $\mu_E = 2$.

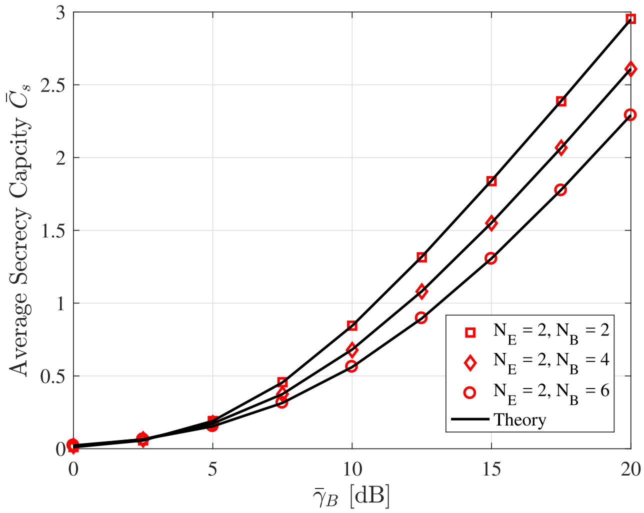


**FIGURE 10.** $\bar{C}_s$ **versus** $\bar{\gamma}_B$ **for selected** $N_B$ **when** $\alpha_B = 3$, $\alpha_E = 4$, $\mu_B = 2$, $\mu_E = 3$, **and** $\bar{\gamma}_E = 5$**dB.**

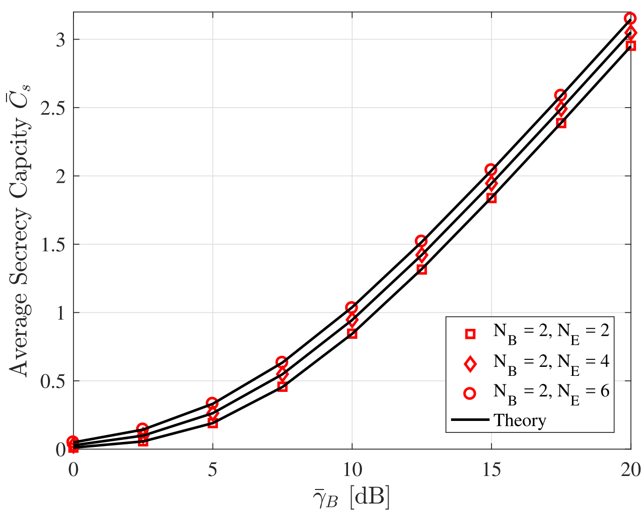


**FIGURE 11.** $\bar{C}_s$ **versus** $\bar{\gamma}_B$ **for selected** $N_E$ **when** $\alpha_B = 3$, $\alpha_E = 4$, $\mu_B = 2$, $\mu_E = 3$, **and** $\bar{\gamma}_E = 5$**dB.**

### B. SECRECY ANALYSIS OVER CASCADED $\alpha$-$\mu$ WIRETAP FADING CHANNELS

In the presence of an active eavesdropper, the secrecy outage probability, the probability of non-zero secrecy capacity, and the average secrecy capacity are presented in this subsection. Fig. 7 plots the secrecy outage probability $\mathcal{P}_{out}$ against the average transmitted power $\bar{\gamma}_B$ when fixing $N_B$ and $N_E$ for selected values. From this figure, it is observed that $\mathcal{P}_{out}$ decreases with the increase of $\bar{\gamma}_B$, which is due to a better secrecy capacity which can be achieved with the increase of $\bar{\gamma}_B$. In addition, the secrecy outage probability is, as expected, strongly influenced by the value of $N_B$ and $N_E$, namely, the number of relays or keyholes. Naturally, this phenomenon can be explained via the fact that more keyholes mean much severer propagation on the legitimate signals.

Additionally, as shown in Fig. 8, our derived asymptotic expression, the $\mathcal{P}_{out}^{Asy}$ given in (40), closely approximates the exact secrecy outage probability $\mathcal{P}_{out}$, in particular, the gap between them is becoming smaller as $\bar{\gamma}_E$ increases.

In Fig. 9, we compare our analytical $\mathcal{P}_{nz}$ given in (47) with Monte-Carlo simulation results. On the contrary with $\mathcal{P}_{out}$, positive secrecy capacity can be surely guaranteed with a higher probability as $\bar{\gamma}_B$ increases.

In Figs. 10 and 11, the average secrecy capacity against $\bar{\gamma}_B$ is presented for two case: (i) selected values of $N_B$; (ii) selected values of $N_E$; An obvious conclusion can be summarized from Figs. 10 and 11 that: the average secrecy capacity is improved with the increase of $N_E$ and degraded with the increase of $N_B$. This is due to the fact, i.e., the bigger $N_B$ (or $N_E$), the worse quality of the received SNR of Bob (or Eve).

Overall, interesting observations drawn from Figs. 7 and 9 can be summarized as follows (i) our analytical results given by (39), (47), and (50) are successfully verified by Monte-Carlo simulation outcomes; (ii) no matter for the $\mathcal{P}_{out}$ or $\mathcal{P}_{nz}$, the number of keyholes or relays is of great significance with the system security performance.

## VI. CONCLUSION AND FUTURE WORK

In this paper, the notion of $N * (\alpha - \mu)$ cascaded fading channels was introduced, together with its statistics characteristics. As stated in the context, it can be respectively reduced to the cascaded Rayleigh, Weibull, Nakagami-*m* fading channels by attributing $\alpha$ and $\mu$ to specific values.

Based on such a general channel model, we further investigated one wireless multi-hop AF relaying link when considering two scenarios: in the absence and presence of an active eavesdropper. Regarding the former scenario, the outage probability, average channel capacity and the ASEP were deduced with closed-form expressions, which were derived in terms of the Fox's $H$-function. When it comes to the latter case, we studied such a digital communication system from the information theoretical perspective. The secrecy metrics, including the secrecy outage probability, the probability of non-zero secrecy capacity, and average secrecy capacity were evaluated, which were correspondingly given with respect to the bivariate and univariate Fox's $H$-function. In addition, the asymptotic analysis of the secrecy outage probability was also derived and therefore compared with the exact expression. Subsequently, our analytical mathematical representations for both cases were further successfully verified via the Monte-Carlo simulation outcomes.

As readily observed from our work, it is so far limited to the investigations of digital wireless communication systems under the assumptions of independent $N * (\alpha - \mu)$ fading channels, generally speaking, one possible future research direction may be the extension of our results to the correlated cascaded $N * (\alpha - \mu)$ fading channels.

## APPENDIX A
## PROOF FOR ASYMPTOTIC $\mathcal{P}_{op}$

Rewrite (16) in terms of the Fox's $H$-function, we have

$$\mathcal{P}_{op} = 1 - \frac{\mathcal{K}_N}{2\pi \mathcal{C} j}\int_{\mathcal{L}} \underbrace{\frac{\Gamma(s)\prod_{k=1}^{N}\Gamma\left(\mu_i + \frac{2}{\alpha_k}s\right)}{\Gamma(1+s)\left(\mathcal{K}_N\gamma_{th}\right)^s}}_{\varepsilon(s)} ds. \quad (51)$$

According to [10], expansions of the univariate and bivariate Fox's $H$-functions can be derived by evaluating the residue of the corresponding integrands at the closest poles to the contour, namely, the minimum pole on the right for large Fox's $H$-function arguments and the maximum pole on the left for small ones.

When $\mathcal{K}_N\gamma_{th} \to \infty$, then applying the residue method given in [10, Sec. IV], one can obtain

$$\begin{aligned}\mathcal{P}_{op} &\approx 1 - \frac{\mathcal{K}_N}{\mathcal{C}}\text{Res}[\varepsilon(s), 0] \\ &= 1 - \lim_{s\to 0} su(s) = 1 - \frac{\mathcal{K}_N}{\mathcal{C}}\prod_{k=1}^{N}\Gamma(\mu_k). \quad (52)\end{aligned}$$

## APPENDIX B
## PROOF FOR THEOREM 5

Revisiting (37) and using the Parseval's relation for Mellin transform [38, eq. (8.3.23)], we have

$$\begin{aligned}\mathcal{I} &= \int_0^\infty \bar{F}_B(\gamma_0) f_E(\gamma_E)d\gamma_E \\ &= \frac{1}{2\pi j}\int_{\mathcal{L}_1}\mathcal{M}[\bar{F}_B(\gamma_0), 1-s]\mathcal{M}[f_E(\gamma_E), s]ds. \quad (53)\end{aligned}$$

where $\mathcal{L}_1$ is the integration path from $\upsilon - j\infty$ to $\upsilon + j\infty$, and $\upsilon$ is a constant [38] Then by introducing the definition of univariate Fox's $H$-function, $\mathcal{M}[\bar{F}_B(\gamma_0), 1-s]$ can be rewritten as

$$\begin{aligned}&\mathcal{M}[\bar{F}_B(\gamma_0), 1-s] \\ &= \int_0^\infty \gamma_E^{-s} F_B(\gamma_0)d\gamma_E \\ &\overset{(c)}{=} \frac{\mathcal{K}_{N_B}}{2\mathcal{C}_{N_B}\pi j}\int_{\mathcal{L}_2}\frac{\Gamma(\xi)\prod_{i=1}^{N_B}\Gamma(\mu_{B,i} + \frac{2}{\alpha_{B,i}}\xi)}{\Gamma(1+\xi)\mathcal{C}_{N_B}^{\xi}}\int_0^\infty \frac{\gamma_E^{-s}}{\gamma_0^{\xi}}d\gamma_E d\xi, \\ &\hspace{20em}(54)\end{aligned}$$

where step $(c)$ is developed by interchanging the order of two integrals.

The inner integral in (54) can be further written as

$$\begin{aligned}\int_0^\infty \gamma_E^{-s}\gamma_0^{-\xi}d\gamma_E &\overset{(d)}{=} \mathcal{W}^{-\xi}\int_0^\infty \frac{\gamma_E^{-s}}{\left(1+\frac{R_s}{\mathcal{W}}\gamma_E\right)^{\xi}}d\gamma_E \\ &\overset{(e)}{=} \mathcal{W}^{-\xi}\mathcal{B}(1-s, \xi+s-1)\left(\frac{R_s}{\mathcal{W}}\right)^{s-1} \\ &\overset{(f)}{=} \mathcal{W}^{-\xi}\frac{\Gamma(1-s)\Gamma(\xi+s-1)}{\Gamma(\xi)}\left(\frac{R_s}{\mathcal{W}}\right)^{s-1}, \\ &\hspace{15em}(55)\end{aligned}$$

where step $(d)$ is developed by representing $\gamma_0 = R_s\gamma_E + \mathcal{W}$, step $(e)$ is obtained from [37, eq. (3.194.3)], and step $(f)$ is further simplified in a closed-form by deploying the property $\mathcal{B}(x, y) = \frac{\Gamma(x)\Gamma(y)}{\Gamma(x+y)}$ [37, eq. (8.384.1)].

Next, plugging (55) into (54), yields the following result

$$\begin{aligned}&\mathcal{M}[\bar{F}_B(\gamma_0), 1-s] \\ &= \frac{\mathcal{K}_{N_B}}{2\mathcal{C}_{N_B}\pi j}\left(\frac{R_s}{\mathcal{W}}\right)^{s-1}\Gamma(1-s) \\ &\quad\times\int_{\mathcal{L}}\frac{\Gamma(\xi+s-1)\prod_{i=1}^{N_B}\Gamma(\mu_{B,i}+\frac{2}{\alpha_{B,i}}\xi)}{\Gamma(1+\xi)}(\lambda_B\mathcal{W})^{-\xi}d\xi \\ &\overset{(g)}{=} \frac{\mathcal{K}_{N_B}\Gamma(1-s)R_s^{s-1}}{\mathcal{C}_{N_B}\mathcal{W}^{s-1}} \\ &\quad\times H_{1,N_B+1}^{N_B+1,0}\left[\mathcal{C}_{N_B}\mathcal{W}\middle|\begin{matrix}(1,1)\\(s-1,1),\theta_1,\cdots,\theta_{N_B}\end{matrix}\right], \quad (56)\end{aligned}$$

where step $(g)$ is directly achieved from the definition of Fox's $H$-function.

Subsequently, substituting (56) and $\mathcal{M}[f_E(\gamma_E), s]$ into (53), where $\mathcal{M}[f_E(\gamma_E), s]$ is given by [46, eq. (5)]

$$\mathcal{M}[f_E(\gamma_E), s] = \mathcal{C}_{N_E} \frac{\prod_{i=1}^{N_E} \Gamma\left(\mu_{E,i} - \frac{2}{\alpha_{E,i}} + \frac{2}{\alpha_{E,i}} s\right)}{\mathcal{C}_{N_E}^s}, \quad (57)$$

results in the following result

$$\mathcal{I} = -\frac{\mathcal{K}_{N_B}\mathcal{K}_{N_E}\mathcal{W}}{4\mathcal{C}_{N_B}R_s\pi^2} \int_{\mathcal{L}_1}\int_{\mathcal{L}_2} \frac{\Gamma(\xi+s-1)\prod_{i=1}^{N_B}\Gamma(\mu_{B,i}+\frac{2}{\alpha_{B,i}}\xi)}{\Gamma(1+\xi)(\mathcal{C}_{N_B}\mathcal{W})^{\xi}} \times \Gamma(1-s)\prod_{i=1}^{N_E}\Gamma\left(\mu_{E,i}-\frac{2}{\alpha_{E,i}}+\frac{2}{\alpha_{E,i}}s\right)\left(\frac{R_s}{\mathcal{C}_{N_E}\mathcal{W}}\right)^s d\xi ds. \quad (58)$$

Finally, plugging (58) in (37) and subsequently applying the bivariate Fox's $H$-function [28, eq. (2.57)], the proof is eventually achieved.

## APPENDIX C
## PROOF FOR ASYMPTOTIC $\mathcal{P}_{out}$

In the case of $\bar{\gamma}_E \to \infty$, we have $\frac{R_s}{\mathcal{C}_{N_E}\mathcal{W}} \to \infty$. The bivariate Fox's $H$-function is evaluated at the highest poles on the left of $\mathcal{L}_1$, i.e., $s = 1-\xi$, by using the residue approach [10], therefore, it leads to the following result,

$$\begin{aligned}
&\frac{1}{2\pi j}\int_{\mathcal{L}_1} \underbrace{\Gamma(\xi+s-1)\Gamma(1-s) \times \prod_{i=1}^{N_E}\Gamma\left(\mu_{E,i}-\frac{2}{\alpha_{E,i}}+\frac{2}{\alpha_{E,i}}s\right)\left(\frac{R_s}{\mathcal{C}_{N_E}\mathcal{W}}\right)^s}_{\psi(s)} ds \\
&\approx \mathrm{Res}[\psi(s), 1-\xi] = \lim_{s\to 1-\xi}(s+\xi-1)\psi(s) \\
&= \Gamma(\xi)\prod_{i=1}^{N_E}\Gamma\left(\mu_{E,i}-\frac{2}{\alpha_{E,i}}\xi\right)\left(\frac{R_s}{\mathcal{C}_{N_E}\mathcal{W}}\right)^{1-\xi}. \quad (59)
\end{aligned}$$

Therefore, we have

$$\mathcal{P}_{out} \approx 1 - \frac{\mathcal{K}_{N_B}\mathcal{K}_{N_E}}{2\pi\mathcal{C}_{N_B}\mathcal{C}_{N_E}j} \times \int_{\mathcal{L}_2} \underbrace{\frac{\Gamma(\xi)\prod_{i=1}^{N_E}\Gamma\left(\mu_{E,i}-\frac{2}{\alpha_{E,i}}\xi\right)\prod_{i=1}^{N_B}\Gamma\left(\mu_{B,i}+\frac{2}{\alpha_{B,i}}\xi\right)}{\Gamma(1+\xi)\left(\frac{\mathcal{C}_{N_B}R_s}{\mathcal{C}_{N_E}}\right)^{\xi}}}_{\tau(\xi)} d\xi, \quad (60)$$

continuation (60) can be successively and asymptotically simplified as (10) by computing the highest pole on the right of the contour $\mathcal{L}_2$, namely $\xi = \frac{\alpha_{E,k}\mu_{E,k}}{2}$, where $\alpha_{E,k}\mu_{E,k} = \min(\alpha_{E,1}\mu_{E,1}, \cdots, \alpha_{E,j}\mu_{E,j}), j = 1, \cdots, N_E$.

$$\mathcal{P}_{out} \approx 1 - \frac{\mathcal{K}_{N_B}\mathcal{K}_{N_E}}{\mathcal{C}_{N_B}\mathcal{C}_{N_E}} \mathrm{Res}\left[\tau(\xi), \frac{\alpha_{E,k}\mu_{E,k}}{2}\right], \quad (61)$$

then making some simple manipulations, the proof for (43) is achieved.

Following the same methodology, the proof for the case, $\bar{\gamma}_B \to \infty$, can be similarly achieved by first computing (58) at the highest pole of $\mathcal{L}_2$ at $\xi = 1-s$, and subsequently evaluating the obtained result at the poles of $\mathcal{L}_1$, i.e., $s = 0$ and $s = \frac{\alpha_{B,k}\mu_{B,k}}{2}$, where $\alpha_{B,k}\mu_{B,k} = \min(\alpha_{B,1}\mu_{B,1}, \cdots, \alpha_{B,i}\mu_{B,i}), i = 1, \cdots, N_B$, respectively.

When $\bar{\gamma}_E \to 0$, the asymptotic $\mathcal{P}_{out}$ is computed at the pole of $\mathcal{L}_1$, i.e., $s = 1$. For the case $\bar{\gamma}_B \to 0$, no pole exists on the right of the contour $\mathcal{L}_2$, $\mathcal{I}$ is directly equal to 1.

## APPENDIX D
## PROOF FOR THEOREM 7

For the ease of deriving the average secrecy capacity, the CDFs of $\gamma_B$ and $\gamma_E$ can be equivalently rewritten as follows

$$\begin{aligned}
\mathcal{I}_1 &= \frac{\mathcal{K}_{N_B}\mathcal{K}_{N_E}}{\ln(2)\mathcal{C}_{N_E}}\int_0^{\infty} H_{2,2}^{1,2}\left[\gamma_B \middle| \begin{matrix}(1,1)(1,1))\\(1,1),(0,1))\end{matrix}\right] H_{0,N_B}^{N_B,0}\left[\mathcal{C}_{N_B}\gamma_B \middle| \begin{matrix}-\\ \Phi_1,\cdots,\Phi_{N_B}\end{matrix}\right] H_{1,N_E+1}^{N_E,1}\left[\mathcal{C}_{N_E}\gamma_B \middle| \begin{matrix}(1,1)\\ \theta_1,\cdots,\theta_{N_E}\end{matrix}\right] d\gamma_B \\
&= \frac{\mathcal{K}_{N_B}\mathcal{K}_{N_E}}{2\pi j\ln(2)\mathcal{C}_{N_E}}\int_{\mathcal{L}_1}\frac{\prod_{l=1}^{N_E}\Gamma\left(\mu_{E,l}-\frac{2s}{\alpha_{E,l}}\right)\Gamma(s)}{\Gamma(1+s)\mathcal{C}_{N_E}^{-s}} \underbrace{\int_0^{\infty}\gamma_B^s H_{2,2}^{1,2}\left[\gamma_B \middle| \begin{matrix}(1,1),(1,1))\\(1,1),(0,1)\end{matrix}\right] H_{0,N_B}^{N_B,0}\left[\mathcal{C}_{N_B}\gamma \middle| \begin{matrix}-\\ \Phi_1,\cdots,\Phi_{N_B}\end{matrix}\right] d\gamma_B}_{U} ds,
\end{aligned} \quad (69)$$

$$\mathcal{I}_1 = -\frac{\mathcal{K}_{N_B}\mathcal{K}_{N_E}}{4\pi^2\ln(2)\mathcal{C}_{N_B}\mathcal{C}_{N_E}}\int_{\mathcal{L}_1}\int_{\mathcal{L}_2}\prod_{i=1}^{N_B}\Gamma\left(m_{B,i}+\frac{2s}{\alpha_{B,i}}+\frac{2t}{\alpha_{B,i}}\right)\frac{\prod_{l=1}^{N_E}\Gamma\left(\mu_{E,l}-\frac{2s}{\alpha_{E,l}}\right)\Gamma(s)\Gamma(1-t)\Gamma^2(t)}{\Gamma(1+s)\Gamma(1+t)\mathcal{C}_{N_B}^t}\left(\frac{\mathcal{C}_{N_E}}{\mathcal{C}_{N_B}}\right)^s dtds, \quad (71)$$

by using [39, eq. (3.9)]

$$F_B(\gamma_B) = \frac{\mathcal{K}_{N_B}}{\mathcal{C}_{N_B}} H^{N_B,1}_{1,N_B+1}\left[\mathcal{C}_{N_B}\gamma \,\middle|\, \begin{matrix} (1,1) \\ \phi_1,\cdots,\phi_{N_B},(0,1) \end{matrix}\right], \tag{62a}$$

$$F_E(\gamma_E) = \frac{\mathcal{K}_{N_E}}{\mathcal{C}_{N_E}} H^{N_E,1}_{1,N_E+1}\left[\mathcal{C}_{N_E}\gamma \,\middle|\, \begin{matrix} (1,1) \\ \theta_1,\cdots,\theta_{N_E},(0,1) \end{matrix}\right], \tag{62b}$$

Recalling the result given in [35], the ASC given in (36) can be further mathematically expressed as

$$\begin{aligned}\bar{C}_s &= \int_0^\infty \int_0^\infty C_s(\gamma_B,\gamma_E) f_{\gamma_B}(\gamma_B) f_{\gamma_E}(\gamma_E) d\gamma_B d\gamma_E \\ &= \mathcal{I}_1 + \mathcal{I}_2 - \mathcal{I}_3,\end{aligned} \tag{63}$$

where

$$\mathcal{I}_1 = \int_0^\infty \log_2(1+\gamma_B) f_B(\gamma_B) F_E(\gamma_B) d\gamma_B, \tag{64}$$

$$\mathcal{I}_2 = \int_0^\infty \log_2(1+\gamma_E) f_E(\gamma_E) F_B(\gamma_E) d\gamma_E, \tag{65}$$

$$\mathcal{I}_3 = \int_0^\infty \log_2(1+\gamma_E) f_E(\gamma_E) d\gamma_E. \tag{66}$$

Next, re-expressing the logarithm function in terms of the Meijer's $G$-function [41], i.e.,

$$\log_2(1+x) = \frac{1}{\ln 2} G^{1,2}_{2,2}\left[x \,\middle|\, \begin{matrix} (1,1) \\ (1,0) \end{matrix}\right], \tag{67}$$

and then using [41, Eq. (8.3.2.21)]

$$H^{m,n}_{p,q}\left[x \,\middle|\, \begin{matrix} (a_p,1) \\ (b_q,1) \end{matrix}\right] = G^{m,n}_{p,q}\left[x \,\middle|\, \begin{matrix} (a_p) \\ (b_q) \end{matrix}\right], \tag{68}$$

$\mathcal{I}_1$ can be rewritten in (69), as shown at the bottom of the page, where $\mathcal{L}_1$ is a certain contour separating the poles of $\prod_{l=1}^{N_E} \Gamma(\mu_{E,l} - s)$ from the poles of $\Gamma(s)$. The inner integral $U$ can be directly developed by using the Mellin transform for the product of two Fox's $H$-functions [41, eq. (2.25.1.1)] as follows

$$U = \mathcal{C}^{s+1}_{N_B} H^{1,2+N_B}_{2+N_B,2}\left[\frac{1}{\mathcal{C}_{N_B}} \,\middle|\, \begin{matrix} (1,1),(1,1),\omega_1,\cdots,\omega_{N_B} \\ (1,1),(0,1) \end{matrix}\right], \tag{70}$$

where $\omega_i = (1-\mu_{B,i} - \frac{2s}{\alpha_{B,i}}, \frac{2}{\alpha_{B,i}})$, subsequently, rewriting (70) in terms of the definition of Fox's $H$-function, then substituting the obtained result into (69), leads to the result given in (71), as shown at the bottom of the page, where $\mathcal{L}_2$ is another contour, next recognizing the definition of bivariate Fox's $H$-functions [28], the proof for $\mathcal{I}_1$ is accomplished.

Similarly, following the same methodology, the proof for $\mathcal{I}_2$ is achieved.

With the help of [41, eq. (2.25.1.1)], the proof for $\mathcal{I}_3$ can be similarly obtained.

## ACKNOWLEDGMENT

The authors would like to thank Dr. H. Chergui for his help.

## REFERENCES

[1] G. K. Karagiannidis, N. C. Sagias, and P. T. Mathiopoulos, "$N$*Nakagami: A novel stochastic model for cascaded fading channels," *IEEE Trans. Commun.*, vol. 55, no. 8, pp. 1453–1458, Aug. 2007.

[2] F. Yilmaz and M.-S. Alouini, "Product of the powers of generalized Nakagami-*m* variates and performance of cascaded fading channels," in *Proc. IEEE Global Telecommun. Conf.*, Nov. 2009, pp. 1–8.

[3] K. Peppas, F. Lazarakis, A. Alexandridis, and K. Dangakis, "Cascaded generalised-K fading channel," *IET Commun.*, vol. 4, no. 1, pp. 116–124, 2010.

[4] N. C. Sagias and G. S. Tombras, "On the cascaded Weibull fading channel model," *J. Franklin Inst.*, vol. 344, pp. 1–11, Jan. 2007.

[5] I. Trigui, A. Laourine, S. Affes, and A. Stephenne, "On the performance of cascaded generalized K fading channels," in *Proc. IEEE Global Telecommun. Conf.*, Nov. 2009, pp. 1–5.

[6] Z. Zheng, "Statistical analysis of cascaded multipath fading channels," Ph.D. dissertation, Dept. Commun. Netw., Aalto Univ., Helsinki, Finland, 2015, pp. 62–64. [Online]. Available: http://urn.fi/URN:ISBN:978-952-60-6563-2

[7] A.-A. A. Boulogeorgos, P. C. Sofotasios, B. Selim, S. Muhaidat, G. K. Karagiannidis, and M. Valkama, "Effects of RF impairments in communications over cascaded fading channels," *IEEE Trans. Veh. Technol.*, vol. 65, no. 11, pp. 8878–8894, Nov. 2016.

[8] N. Hajri, N. Youssef, T. Kawabata, M. Pätzold, and W. Dahech, "Statistical properties of double Hoyt fading with applications to the performance analysis of wireless communication systems," *IEEE Access*, vol. 6, p. 19597–19609, 2018.

[9] H. Ilhan, "Performance analysis of two-way AF relaying systems over cascaded Nakagami-*m* fading channels," *IEEE Signal Process. Lett.*, vol. 19, no. 6, pp. 332–335, Jun. 2012.

[10] H. Chergui, M. Benjillali, and S. Saoudi, "Performance analysis of project-and-forward relaying in mixed MIMO-pinhole and Rayleigh dual-hop channel," *IEEE Commun. Lett.*, vol. 20, no. 3, pp. 610–613, Mar. 2016.

[11] B. Talha and M. Pätzold, "Channel models for mobile-to-mobile cooperative communication systems: A state of the art review," *IEEE Veh. Technol. Mag.*, vol. 6, no. 2, pp. 33–43, Jun. 2011.

[12] V. Erceg, S. J. Fortune, J. Ling, A. J. Rustako, and R. A. Valenzuela, "Comparisons of a computer-based propagation prediction tool with experimental data collected in urban microcellular environments," *IEEE J. Sel. Areas Commun.*, vol. 15, no. 4, pp. 677–684, May 1997.

[13] A. Bekkali, S. Zou, A. Kadri, M. Crisp, and R. V. Penty, "Performance analysis of passive UHF RFID systems under cascaded fading channels and interference effects," *IEEE Trans. Wireless Commun.*, vol. 14, no. 3, pp. 1421–1433, Mar. 2015.

[14] P. C. Sofotasios, L. Mohjazi, S. Muhaidat, M. Al-Qutayri, and G. K. Karagiannidis, "Energy detection of unknown signals over cascaded fading channels," *IEEE Antennas Wireless Propag. Lett.*, vol. 15, pp. 135–138, May 2016.

[15] Y. Alghorani, G. Kaddoum, S. Muhaidat, S. Pierre, and N. Al-Dhahir, "On the performance of multihop-intervehicular communications systems over n*Rayleigh fading channels," *IEEE Wireless Commun. Lett.*, vol. 5, no. 2, pp. 116–119, Apr. 2016.

[16] A. Laourine, M.-S. Alouini, S. Affes, and A. Stephenne, "On the performance analysis of composite multipath/shadowing channels using the G-distribution," *IEEE Trans. Commun.*, vol. 57, no. 4, pp. 1162–1170, Apr. 2009.

[17] N. Hajri, N. Youssef, and M. Pätzold, "On the statistical properties of phase crossings and random FM noise in double Rayleigh fading channels," *IEEE Trans. Veh. Technol.*, vol. 65, no. 4, pp. 1859–1867, Apr. 2016.

[18] M. D. Yacoub, "The $\alpha$-$\mu$ distribution: A physical fading model for the Stacy distribution," *IEEE Trans. Veh. Technol.*, vol. 56, no. 1, pp. 27–34, Jan. 2007.

[19] Q. Wu, D. W. Matolak, and I. Sen, "5-GHz-band vehicle-to-vehicle channels: Models for multiple values of channel bandwidth," *IEEE Trans. Veh. Technol.*, vol. 59, no. 5, pp. 2620–2625, Jun. 2010.

[20] A. Michalopoulou *et al.*, "Statistical analysis for on-body spatial diversity communications at 2.45 GHz," *IEEE Trans. Antennas Propag.*, vol. 60, no. 8, pp. 4014–4019, Aug. 2012.

[21] A. M. Mathai, "Products and ratios of generalized gamma variates," *Skandinavisk Aktuarietidskrif*, no. 2, pp. 193–198, 1972.

[22] E. J. Leonardo and M. D. Yacoub, "The product of two $\alpha$-$\mu$ variates and the composite $\alpha$-$\mu$ multipath–shadowing model," *IEEE Trans. Veh. Technol.*, vol. 64, no. 6, pp. 2720–2725, Jun. 2015.
[23] E. J. Leonardo and M. D. Yacoub, "Product of $\alpha$-$\mu$ variates," *IEEE Wireless Commun. Lett.*, vol. 4, no. 6, pp. 637–640, Dec. 2015.
[24] O. S. Badarneh and F. S. Almehmadi, "Performance of multihop wireless networks in $\alpha$-$\mu$ fading channels perturbed by an additive generalized Gaussian noise," *IEEE Commun. Lett*, vol. 20, no. 5, pp. 986–989, May 2016.
[25] O. S. Badarneh, "The $\alpha$-$\mu$/$\alpha$-$\mu$ composite multipath-shadowing distribution and its connection with the extended generalized-K distribution," *AEU-Int. J. Electron. Commun.*, vol. 70, no. 9, pp. 1211–1218, 2016. [Online]. Available: http://www.sciencedirect.com/science/article/pii/S1434841116302254
[26] E. J. Leonardo, M. D. Yacoub, and R. A. A. de Souza, "Ratio of products of $\alpha$-$\mu$ variates," *IEEE Commun. Lett.*, vol. 20, no. 5, pp. 1022–1025, May 2016.
[27] C. R. N. da Silva, E. J. Leonardo, and M. D. Yacoub, "Product of two envelopes taken from $\alpha$-$\mu$, $\kappa$-$\mu$, and $\eta$-$\mu$ distributions," *IEEE Trans. Commun.*, vol. 66, no. 3, pp. 1284–1295, Mar. 2018.
[28] A. M. Mathai, R. K. Saxena, and H. J. Haubold, *The H-Function: Theory and Applications*. Springer, 2009.
[29] I. S. Ansari, F. Yilmaz, and M.-S. Alouini, "On the sum of squared $\eta - \mu$ random variates with application to the performance of wireless communication systems," in *Proc. IEEE 77th VTC Spring*, Jun. 2013, pp. 1–6.
[30] K. P. Peppas, F. Lazarakis, A. Alexandridis, and K. Dangakis, "Simple, accurate formula for the average bit error probability of multiple-input multiple-output free-space optical links over negative exponential turbulence channels," *Opt. lett.*, vol. 37, no. 15, pp. 3243–3245, 2012.
[31] K. P. Peppas, "A new formula for the average bit error probability of dual-hop amplify-and-forward relaying systems over generalized shadowed fading channels," *IEEE Wireless Commun. Lett.*, vol. 1, no. 2, pp. 85–88, Apr. 2012.
[32] A. D. Wyner, "The wire-tap channel," *Bell Syst. Tech. J.*, vol. 54, no. 8, pp. 1355–1387, 1975.
[33] H. Lei, C. Gao, Y. Guo, and G. Pan, "On physical layer security over generalized Gamma fading channels," *IEEE Commun. Lett.*, vol. 19, no. 7, pp. 1257–1260, Jul. 2015.
[34] L. Kong, H. Tran, and G. Kaddoum, "Performance analysis of physical layer security over $\alpha$-$\mu$ fading channel," *Electron. Lett.*, vol. 52, no. 1, pp. 45–47, 2016.
[35] H. Lei, I. S. Ansari, G. Pan, B. Alomair, and M.-S. Alouini, "Secrecy capacity analysis over $\alpha$–$\mu$ fading channels," *IEEE Commun. Lett.*, vol. 21, no. 6, pp. 1445–1448, Jun. 2017.
[36] L. Kong, G. Kaddoum, and Z. Rezki, "Highly accurate and asymptotic analysis on the SOP over SIMO $\alpha - \mu$ fading channels," *IEEE Commun. Lett.*, to be published.
[37] I. S. Gradshteyn and I. M. Ryzhik, *Table of Integrals, Series, and Products*. New York, NY, USA: Academic, 2014.
[38] L. Debnath and D. Bhatta, *Integral Transforms and Their Applications*, vol. 3. Boca Raton, FL, USA: CRC Press, 2014.
[39] C. D. Bodenschatz, "Finding an H-function distribution for the sum of independent H-function variates," Ph.D. dissertation, Univ. Texas Austin, Austin, TX, USA, 1992.
[40] WAFO-Group, "WAFO—A MATLAB toolbox for analysis of random waves and loads—A tutorial," Dept. Math. Statist., Center Math. Sci., Lund Univ., Lund, Sweden, Tech. Rep., 2000.
[41] A. P. Prudnikov, Y. A. Brychkov, and O. I. Marichev, *Integrals and Series: More Special Functions*, vol. 3. Gordon and Breach Science Publishers, 1990.
[42] O. S. Badarneh and M. S. Aloqlah, "Performance analysis of digital communication systems over $\alpha$–$\eta$–$\mu$ fading channels," *IEEE Trans. Veh. Technol.*, vol. 65, no. 10, pp. 7972–7981, Oct. 2016.
[43] M. Bloch, J. Barros, M. R. D. Rodrigues, and S. W. McLaughlin, "Wireless information-theoretic security," *IEEE Trans. Inf. Theory*, vol. 54, no. 6, pp. 2515–2534, Jun. 2008.
[44] L. Kong, J. He, G. Kaddoum, S. Vuppala, and L. Wang, "Secrecy analysis of a MIMO full-duplex active eavesdropper with channel estimation errors," in *Proc. IEEE 84th VTC-Fall*, Sep. 2016, pp. 1–5.
[45] *Wolfram Language & System Documentation Center*. [Online]. Available: http://reference.wolfram.com/language/ref/MeijerG.html
[46] H. R. Alhennawi, M. M. H. E. Ayadi, M. H. Ismail, and H.-A. M. Mourad, "Closed-form exact and asymptotic expressions for the symbol error rate and capacity of the $H$-function fading channel," *IEEE Trans. Veh. Technol.*, vol. 65, no. 4, pp. 1957–1974, Apr. 2016.

**LONG KONG** (GS'18) received the B.S. degree in telecommunication engineering from Hainan University, Haikou, China, in 2010, and the M.S. degree in communication engineering from Xiamen University, Xiamen, China, in 2013. He is currently pursuing the Ph.D. degree in electrical engineering with the École de Technologie Supérieure, Université du Québec. From 2013 to 2014, he was a Research Assistant of electronic and information engineering with The Hong Kong Polytechnic University, Hong Kong. His research interests include physical layer security, cooperative communications, and chaos-based communication systems.

**GEORGES KADDOUM** (M'11) received the bachelor's degree in electrical engineering from the Ecole Nationale Supérieure de Techniques Avancées Bretagne, Brest, France, the M.S. degree in telecommunications and signal processing (circuits, systems, and signal processing) from the Université de Bretagne Occidentale and Telecom Bretagne (ENSTB), Brest, in 2005, and the Ph.D. degree (Hons.) in signal processing and telecommunications from the National Institute of Applied Sciences, University of Toulouse, Toulouse, France, in 2009. Since 2010, he has been a Scientific Consultant in the field of space and wireless telecommunications for several U.S. and Canadian companies. Since 2013, he has been an Assistant Professor of electrical engineering with the Ecole de Technologie Supérieure (ÉTS), University of Quebec, Montréal, QC, Canada. In 2014, he was the ÉTS Research Chair in physical layer security for wireless networks. He has published over 130 journal and conference papers and has two pending patents. His recent research activities cover mobile communication systems, modulations, security, and space communications and navigation.

Dr. Kaddoum received the Best Papers Awards at the 2014 IEEE International Conference on Wireless and Mobile Computing, Networking, Communications, with three co-authors and at the 2017 IEEE International Symposium on Personal Indoor and Mobile Radio Communications, with four co-authors. He received the 2015 and 2017 IEEE Transactions on Communications Exemplary Reviewer Award. He is currently serving as an Associate Editor for IEEE Transactions on Information Forensics and Security, and IEEE Communications Letters.

**DANIEL BENEVIDES DA COSTA** (S'04–M'08–SM'14) was born in Fortaleza, Brazil, in 1981. He received the B.Sc. degree in telecommunications from the Military Institute of Engineering, Rio de Janeiro, Brazil, in 2003, and the M.Sc. and Ph.D. degrees in electrical engineering, area: telecommunications, from the University of Campinas, Campinas-SP, Brazil, in 2006 and 2008, respectively.

From 2008 to 2009, he was a Post-Doctoral Research Fellow with INRS-EMT, University of Quebec, Montreal, QC, Canada. Since 2010, he has been with the Federal University of Ceará, where he is currently an Associate Professor.

Prof. da Costa was a member of the Advisory Board of the Ceará from 2012 to 2017. He acts as a Scientific Consultant of the National Council of Scientific and Technological Development (CNPq), Brazil, and he is a Productivity Research Fellow of CNPq.

Prof. da Costa is a member of the IEEE Communications Society and the IEEE Vehicular Technology Society. He was a recipient of four conference paper awards. He received the Exemplary Reviewer Certificate of the IEEE WIRELESS COMMUNICATIONS LETTERS in 2013, the Exemplary Reviewer Certificate of the IEEE COMMUNICATIONS LETTERS in 2016 and 2017, the Certificate of Appreciation of Top Associate Editor for outstanding contributions to IEEE TRANSACTIONS ON VEHICULAR TECHNOLOGY in 2013, 2015, and 2016, the Exemplary Editor Award of the IEEE COMMUNICATIONS LETTERS in 2016, and the Outstanding Editor Award of the IEEE ACCESS in 2017. He is a Distinguished Lecturer of the IEEE Vehicular Technology Society. His Ph.D. dissertation was awarded the Best Ph.D. Thesis in electrical engineering from the Brazilian Ministry of Education (CAPES) at the 2009 CAPES Thesis Contest. He is currently the Chair of the Special Interest Group on Energy-Harvesting Cognitive Radio Networks in the IEEE Cognitive Networks Technical Committee. He has served as Associate Technical Editor for the *IEEE Communications Magazine*. From 2012 to 2017, he was an Editor of the IEEE COMMUNICATIONS LETTERS. He has also served as an Area Editor for *KSII Transactions on Internet and Information Systems* and a guest editor for several journal special issues. He is an Editor of the IEEE COMMUNICATIONS SURVEYS AND TUTORIALS, the IEEE ACCESS, the IEEE TRANSACTIONS ON COMMUNICATIONS, the IEEE TRANSACTIONS ON VEHICULAR TECHNOLOGY, and *EURASIP Journal on Wireless Communications and Networking*. He has been involved in the organizing committee of several conferences. He is currently a Latin American Chapters Coordinator of the IEEE Vehicular Technology Society.